UNIVERSITY OF TROMSØ UIT

FACULTY OF HEALTH SCIENCES
DEPARTMENT OF MEDICAL BIOLOGY

Structure, function and inhibition of the serotonin transporter studied by molecular docking, -dynamics and virtual screening

Mari Gabrielsen

A dissertation for the degree of
Philosophiae Doctor

June 2011

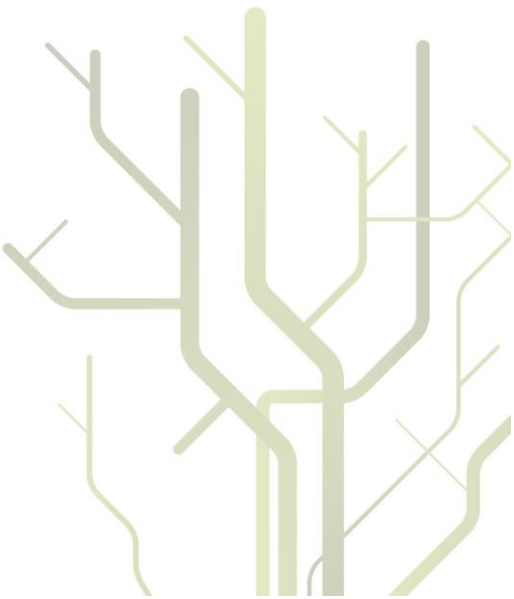

CONTENTS

ACKNOWLEDGEMENTS

This study was carried out at the University of Tromsø from 2007 - 2011 and during four shorter stays in Krakow and Warsaw, Poland. The work was supported by a grant from the Nevronor program of the Research Council of Norway (project 176956/V40), the Polish-Norwegian Research Fund (grant PNRF-103-AI-1/07) and the University of Tromsø.

I would like to thank my supervisors, Professor Ingebrigt Sylte, Dr. Aina W. Ravna, Associate Professor Kurt Kristiansen and Professor Arne Smalås. The work in papers 2-4 would not have been possible without the help of our Polish and American co-operation partners. I would especially like to thank Associate Professor Andrzej J. Bojarski, Professor Zdzisław Chilmonczyk, M. Sc. Rafał Kurczab and their co-workers, and Dr. Irina Kufareva and Professor Ruben Abagyan.

My gratitude is also expressed to the Stallo support team for helping me with my MD simulations at the supercomputer, and to my colleague Dr. Roy A. Lysså for his excellent help on figure 1.

Tromsø, June 2011

Mari Gabrielsen

LIST OF PAPERS

4 papers are attached with the thesis:

1. Substrate binding and translocation of the serotonin transporter studied by docking and molecular dynamics simulations
   Journal of Molecular Modeling, 2011, DOI 10.1007/s00894-011-1133-1
2. Molecular mechanism of serotonin transporter inhibition elucidated by a new flexible docking protocol
   Submitted to *European Journal of Medicinal Chemistry, 2011*
3. Identification of novel serotonin transporter compounds by virtual screening and experimental verification
   Manuscript, 2011
4. Synthesis, docking and antidepressant evaluation of long-chain alkylnitroquipazines, inhibitors of the serotonin transporter
   Manuscript, 2011

ABBREVIATIONS

5-HT	5-Hydroxytryptamine (serotonin)
AR	Aromatic group
DAT	Dopamine transporter
EL	Extracellular loop
GPCR	G-protein coupled receptor
HBA	Hydrogen bond acceptor feature
HBD	Hydrogen bond donor feature
HYD	Hydrophobic region
IL	Intracellular loop
ICM	Internal Co-ordinate Mechanics
LeuT	Leucine transporter
MD	Molecular dynamics
NET	Noradrenaline (norepinephrine) transporter
NSS	Neurotransmitter:sodium symporter
PI	Positive ionisable group
RMSD	Root mean square deviation
SERT	Serotonin transporter
SSRI	Selective serotonin reuptake inhibitor
TCA	Tricyclic antidepressant
TM	Transmembrane α-helix
VS/VLS	Virtual screening/Virtual ligand screening

1. INTRODUCTION

1.1 Pharmacology

Pharmacology is derived from the Greek *pharmakon*, meaning ‘drug’, ‘medicine’ or ‘poison’, and *logia*, ‘study’ and is the study of how chemical agents affect living processes. Though humans have been using drugs for many thousand years, the modern era of pharmacology did not begin before in the early nineteenth century when major advances were made in the fields of chemistry and physiology. In physiology, the understanding of normal physiologic processes increased and led to an understanding of the dynamic actions chemicals have on biological processes and materials. In chemistry, the development of isolation and synthesis methods made natural compounds available and derivatives of natural compounds, or completely new compounds, were synthesised. The first isolation of an active compound of a medical plant took place in 1806 when Frederick W. A. Sertürner (1783-1841) isolated morphine from opium, the dried latex obtained from the poppy *Papaver somniferum*.

During this time, the concept of drug interactions started to form. Felix Fontana (1720-1805) was the first to suggest that crude drugs contain active constituents that interact with one or more discrete parts of the organism to produce their characteristic effects (Levine et al., 2000). This suggestion was 50 years later experimentally confirmed by French physiologist François Magendie (1783-1841). His student Claude Bernard (1813-1878) later concluded that in order to understand the action of a drug, it was essential to know both which tissues primarily were involved and to explain how the drug interacted with the biologic system to produce its effect, and the German pharmacologist Rudolf Buchheim (1820-1879) noted that drug activity could be explained on the basis of physicochemical reactions between cell constituents and the particular drug. Then, at the turn of the twentieth century, John Newport Langley (1852-1925), a British physiologist, and the German scientist Paul Erlich (1854-1915) both postulated that drugs specifically must bind to chemical constituents present in cells (receptors) in order to be active (Levine et al., 2000). Not until the 1960s and -70s, however, did receptors begin to be isolated as specific proteins of the cell membrane and no longer remained hypothetical.

Today, the term receptor (or, more precisely, *drug-target*) is defined as a specialised macromolecule that is able to selectively recognise drugs and, as a consequence of this recognition, set in motion biochemical reactions that ultimately result in biologic response

(Levine et al., 2000). The number of distinct molecular targets for all classes of approved therapeutic drugs was recently found to be 324, of which 266 were human and 58 were microbial, viral, fungal or parasitic in origin (Overington et al., 2006). 50 % of the drugs acted on proteins from one of only four gene families: the rhodopsin-like G-protein coupled receptor (GPCR), nuclear receptor, ligand-gated ion channel or voltage-gated ion channel families. Furthermore, 60 % of the drug targets were membrane proteins, though only 22 % of the genes in the human genome encode such proteins (Overington et al., 2006).

The era of 3D experimental structure determination began in the late 1950s. The first x-ray crystal structure was that of the soluble protein myoglobin, which was solved at 6 Å resolution in 1958 and, two years later, at 2 Å resolution (Kendrew et al., 1958; Kendrew et al., 1960). In 1962, John C. Kendrew, together with Max F. Perutz, received the Nobel Prize in Chemistry 'for their studies of the structures of globular proteins'. Whereas the myoglobin protein was solved in the late 1950s, the first x-ray crystal structure of an integral membrane protein at nearly atomic resolution (3 Å resolution), the photosynthetic reaction centre, was not published before 1985 (Deisenhofer et al., 1985). Experimental structure determination of membrane proteins is very challenging and in 2009, approximately 180 unique membrane proteins x-ray crystal structures had been deposited in the protein data bank (PDB) (White, 2009), of approximately 10.000 unique proteins in total (Abagyan and Kufareva, 2009).

Whereas the era of modern pharmacology began in the early nineteenth century, the revolution of psychopharmacology did not begin until the 1950s, when the tranquilisers (e.g. chlorpromazine) and antidepressant drugs were discovered. Before this, treatment of psychopathologies was mainly non-specific and speculative and e.g. included insulin shock and lobotomy. The two first antidepressant drugs, iproniazid and imipramine - a monoamine oxidase (MAO) inhibitor and a tricyclic antidepressant (TCA), respectively - not only changed the psychiatric care of depressive patients, but also proved to be excellent research tools. In fact, the discovery that the drugs centrally enhanced the levels of monoamines ultimately led to the proposal of the 'monoamine theory of depression', which states that low monoamine levels in certain brain regions leads to depression (Schildkraut, 1965). Though the theory is oversimplified, all currently available antidepressant drugs act on the monoamine system (more specifically, the serotonergic and noradrenergic systems) and the theory still serve as a basis for understanding the action of antidepressants.

1.2 The serotonergic system

The serotonergic system has been implicated in many physiological processes and behaviours such as sleep, thermoregulation, satiety, neurogenesis, stress response and aggression (Russo et al., 2009). Moreover, the system is associated with several psychiatric disorders, including depression, anxiety and obsessive compulsive disorder (Murphy et al., 2004).

In the CNS, serotonergic cell bodies form collections of clustered cells called the raphe nuclei of the lower brainstem, the largest collection being the dorsal raphe. Unlike the cell bodies, however, the serotonergic projections are extensive and innervate practically all parts of the brain and spinal cord (Fuxe et al., 2007). Serotonin (5-hydroxytryptamine, 5-HT) itself is derived from the essential amino acid tryptophan in the presynaptic serotonergic neurons of the CNS. The hydroxylation of tryptophan, catalysed by a tryptophan hydroxylase, yields 5-hydroxytryptophan (5-HTP), which is then decarboxylated by an aromatic amino acid decarboxylase to 5-hydroxytryptamine – 5-HT. After its generation, 5-HT is taken up into storage vesicles and is released from the nerve terminals (upon arrival of nerve impulses) into the synaptic cleft where it may interact with 5-HT receptors located in the membrane of postsynaptic neurons to yield its biological effects (Figure 1). Fifteen different 5-HT receptors belonging to seven main classes of 5-HT receptors have been identified so far. Fourteen of the receptors are G-protein coupled receptors (GPCRs), characterised by their seven transmembrane-spanning α-helices, whereas one, the 5-HT_3 receptor, is an ionotropic receptor, i.e., a ligand-gated ion channel, consisting of five subunits that form an ion conduction pore permeable to Na^+, K^+ and Ca^{2+} ions. Upon activation by 5-HT, the ion channel opens, resulting in an excitatory response in the neuron. In contrast, the effects of activation of the serotonergic GPCRs are mediated through different intracellular signal transduction systems in the postsynaptic neuron.

The serotonin transporter (SERT) plays an important role in the termination of serotonergic neurotransmission by transporting 5-HT from the synaptic cleft into the presynaptic neuron, where it is either recycled into storage vesicles or is converted to an inactive metabolite, 5-hydroxyindolacetic acid (5-HIAA), by the monoamine oxidase (MAO). The serotonergic system is also auto-regulatory: 5-HT activation of 5-HT_{1A} or 5-HT_{1B} receptors located in somatodendritic and nerve terminal regions of the presynaptic neuron, respectively, reduces the amount of 5-HT in the synaptic cleft and hence regulates serotonergic signal transduction (Figure 1).

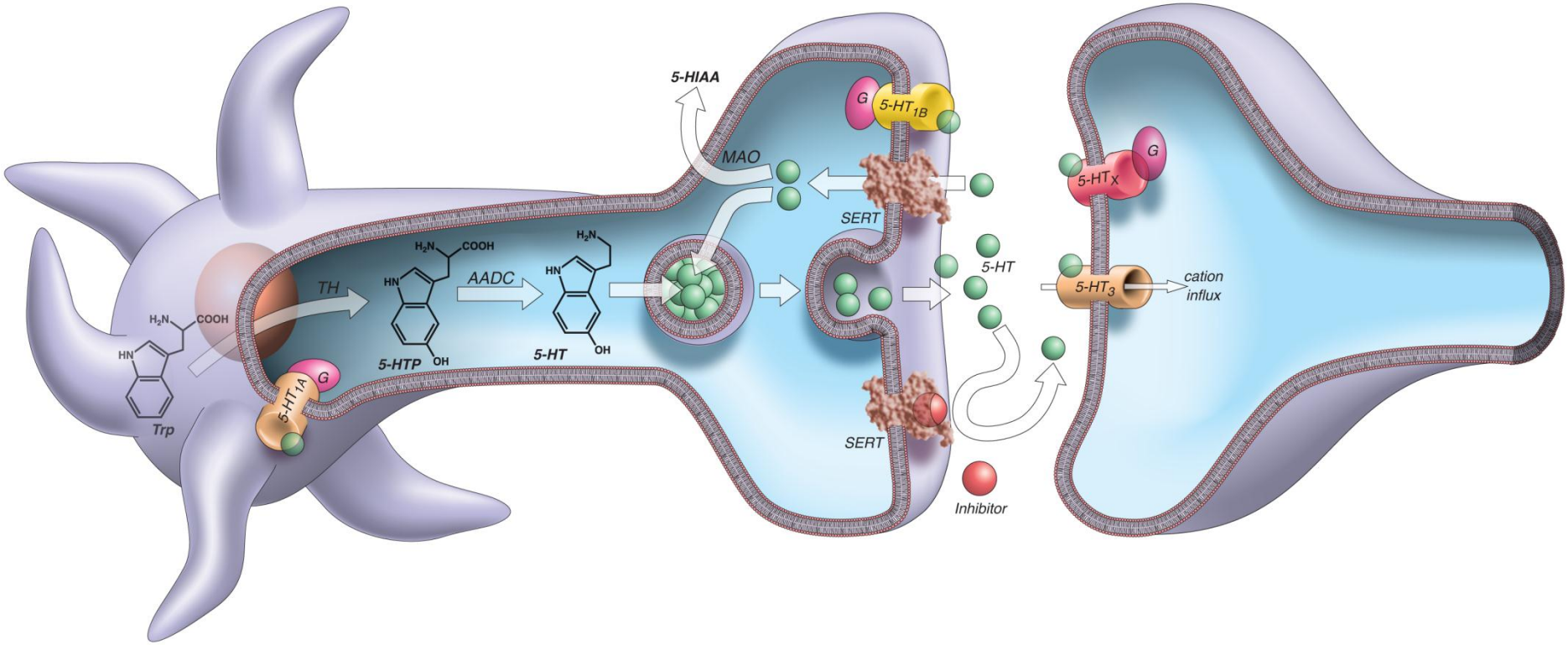

Figure 1. The serotonergic system. *Trp*, tryptophan; *TH*, tryptophan hydroxylase; *5-HTP*, 5-hydroxytryptophan; *AADC*, aromatic amino acid decarboxylase; *5-HT*, 5-hydroxytryptamine (serotonin); *SERT*, serotonin transporter; *MAO*, monoamine oxidase; *5-HIAA*, 5-hydroxyindolacetic acid; 5-HT_x, G-protein coupled 5-HT receptors

1.3 The serotonin transporter (SERT)

1.3.1 SERT classification and function

The serotonin transporter (SERT) belongs to the neurotransmitter:sodium symporter (NSS) family of transporters (transporter classification code 2.A.22) (Saier, 2000), also known as the solute carrier 6 (SLC6) family (Chen et al., 2004). A large number of transporters belong to this family, which contains both eukaryotic and prokaryotic transporters (Beuming et al., 2006). In addition to SERT and the closely related dopamine and noradrenaline (norepinephrine) transporters (DAT and NET, respectively), multiple other transporters, such as the glycine (GlyT), γ-aminobutyric acid (GABA, GAT-1), tryptophan (TnT), tyrosine (Tyt1) and leucine (LeuT) transporters, are classified as NSS transporters. Beuming et al. identified 177 eukaryotic and 167 prokaryotic NSS transporters (sequences with less than 95% identity) (Beuming et al., 2006).

The NSS family members are secondary transporters that couple the potential energy stored in pre-existing ion gradients to the uptake of molecules across the cell membrane against the concentration gradient of the molecule. The alternate access model of substrate translocation states that the centrally located substrate binding site is connected with the intracellular and extracellular environments of the cell through permeation pathways (Jardetzky, 1966; Tanford, 1983). The binding site is only accessible to one permeation pathway at a time; hence, the alternate access model involves a conformational cycle between inward- and outward-facing conformations of the transporter (Jardetzky, 1966; Tanford, 1983). SERT utilises an electrochemical gradient of sodium and chloride ions to transport 5-HT (Rudnick, 1977; Gu et al., 1996; Rudnick, 1998; Rudnick, 2006). 5-HT, Na^+ and Cl^- are transported in a 1:1:1 stoichiometry and all solutes must probably bind before SERT can undergo the conformational changes leading to translocation (Nelson and Rudnick, 1979; Zhang and Rudnick, 2006). Simultaneous efflux of one K^+ ion also takes place (Nelson and Rudnick, 1979).

All members of the NSS family require sodium for transport of their substrates; however, the requirement of chloride varies. The biogenic amine transporters (SERT, DAT and NET) and GAT-1 are strongly Cl^--dependent, whereas LeuT, Tyt1 and Tna1 are Cl^--independent (Forrest et al., 2007). Studies show that mutation of the serine in position 372 in SERT, and amino acids in the equivalent positions in other Cl^--dependent transporters, to

either glutamate or aspartate found in Cl^--independent transporters removes the chloride requirement of the transporters (Forrest et al., 2007; Zomot et al., 2007).

The Na^+ and Cl^- ions also play important roles in inhibitor binding in SERT. Na^+ is known to stimulate the binding of all SERT inhibitors, the only exception being ibogaine, which has been proposed to stabilise an inward-facing SERT and whose affinity increased when Na^+ was removed (Cool et al., 1990; Humphreys et al., 1994; Jacobs et al., 2007; Tavoulari et al., 2009). Some SERT inhibitors are also stimulated by Cl^-, notably imipramine, fluoxetine, citalopram and sertraline, whereas cocaine and paroxetine binding is not affected by Cl^- (Humphreys et al., 1994; Tavoulari et al., 2009).

1.3.2 Drugs interacting with SERT

Together with the other monoamine transporters, DAT and NET, SERT is one of the most studied drug targets in the CNS. In addition to playing a major role in the termination of serotonergic neurotransmission, SERT is targeted by the tricyclic antidepressants (TCA) as well as the newer selective serotonin reuptake inhibitor (SSRI). The transporter is furthermore a target of illicit psychostimulants such as cocaine and amphetamines, including 3,4-methylenedioxy-*N*-methamphetamine (MDMA (‘ecstasy’)) (Rudnick and Wall, 1992). The TCAs are high-affinity binders of both SERT and NET, while SSRIs are high-affinity binders of SERT though also have low affinity to the other monoamine transporters (Owens et al., 1997; Tatsumi et al., 1997; Eshleman et al., 1999). The *in vivo* pharmacological effects of the TCAs and SSRIs appear to be mediated almost exclusively by inhibition of SERT and NET (Zhou et al., 2007).

The current antidepressant drugs, however, have numerous unwanted side effects, including cardiovascular, dermatological, gastrointestinal, neuropsychiatric and genitourinary effects (Omori et al., 2010). Moreover, as many as 2 in 5 may not respond to the currently available antidepressant treatment (Dubovsky and Warren, 2009). The antidepressant effect of TCAs and SSRIs may also take from two to six weeks to develop, an effect most likely due to the autoinhibitory regulation of the serotonergic system. Thus, though multiple antidepressant drug therapies are available today, the need for new antidepressants is still great.

1.3.3 SERT structure

The first 5-HT transporters to be cloned and expressed were from rat and human (Blakely et al., 1991; Ramamoorthy et al., 1993). Multiple other SERT sequences, including fruit fly (*Drosophila melanogaster*), guinea pig, bovine, monkey, chicken, and the parasitic flatworm *Schistosoma mansoni*, have later also been cloned and expressed (Corey et al., 1994; Demchyshyn et al., 1994; Chen et al., 1998b; Mortensen et al., 1999; Miller et al., 2001; Larsen et al., 2004; Patocka and Ribeiro, 2007).

Hydropathy plots and experimental data predict that the 630 amino acid long human SERT contains 12 transmembrane α-helices (TMs) connected by intra- and extracellular loops (ILs and ELs, respectively) and that the N- and C-termini are intracellular (Ramamoorthy et al., 1993; Chen et al., 1998a; Androutsellis-Theotokis and Rudnick, 2002). Strong evidence also suggests that SERT, like most eukaryotic NSS members, functions as a homo-oligomer (Jess et al., 1996; Chang et al., 1998; Kilic and Rudnick, 2000; Schmid et al., 2001; Kocabas et al., 2003; Ozaslan et al., 2003; Just et al., 2004; Fjorback et al., 2009). Furthermore, the homologous prokaryotic leucine transporter (LeuT, see 1.3.4 LeuT crystal structures) was also crystallised as a dimer (Yamashita et al., 2005). In LeuT, the interface between the two protomers are formed by EL2 and TMs 9 and 12, where TMs 9 and 12 of both protomers form a four-helix bundle (Yamashita et al., 2005). TMs 11 and 12 have been indicated to participate in oligomerisation in SERT (Just et al., 2004).

The 3D structure of SERT, or any other eukaryotic NSS transporter, has not been experimentally determined. Overexpression of SERT is required to obtain sufficient material for x-ray crystallisation studies; however, like many other mammalian membrane proteins, SERT cannot be functionally expressed in bacteria or yeast cells, and although functional in mammalian cell lines, SERT expression levels are low and large scale expression and purification is difficult (Tate, 2001; Tate et al., 2003).

1.3.4 LeuT x-ray crystal structures

A major breakthrough in 3D structure determination of NSS members came in 2005 with the x-ray crystallisation of the *Aquifex aeolicus* leucine transporter (LeuT), which was crystallised in complex with its substrate leucine and two sodium ions (Yamashita et al., 2005). The crystal structure shows that the transporter core is made up of the ten first TMs and that TMs 1-5 and 6-10 are pseudosymmetrical (Yamashita et al., 2005). Interestingly,

approximately 70% of the prokaryotic NSS members contain only 11 TMs, and the first functional 11 TM transporter, the tyrosine transporter (Tyt1) from *Fusobacterium nucleatum*, was cloned in 2006 (Quick et al., 2006). The 11 TM NSS transporters all contain TMs 1-11 but not TM12, which hence supports the notion that the first ten TMs constitute the functional core of the NSS transporters.

The substrate binding site of LeuT is located approximately halfway across the membrane and is made up by amino acids from TMs 1, 3, 6 and 8. Moreover, TMs 1 and 6 are partially unwound in this region. Two sodium binding sites (Na1 and Na2) are also located in close proximity to the leucine binding site: the Na1 sodium atom is directly coordinated to the leucine substrate and has been suggested to be cotransported, whereas the Na2 sodium ion has been proposed to play a structural role (Yamashita et al., 2005). The amino acids coordinating the Na1 and Na2 sodium ions are highly conserved and the Na1 and Na2 sodium ion binding sites are most likely present in SERT (Beuming et al., 2006).

LeuT shares an overall sequence identity of 21, 20 and 24% with SERT, DAT and NET, respectively, however, the TMs involved in substrate binding - TMs 1, 3, 6 and 8 –are much more conserved (Beuming et al., 2006). The similarities in sequence as well as in function between LeuT and SERT hence provide the possibility of generating a model of SERT using the LeuT structure. Furthermore, several other LeuT x-ray crystal structures have been published and structures of LeuT in occluded and outward-facing conformations are deposited in the PDB databank (Singh et al., 2007; Zhou et al., 2007; Singh et al., 2008; Zhou et al., 2009). LeuT has also been crystallised with TCAs and SSRIs (see 1.3.5 SERT ligand binding sites).

1.3.5 SERT ligand binding sites

Both the sequence homology to LeuT and mutational studies suggest that the substrate binding site of SERT is located in the region corresponding to the LeuT substrate binding site (Beuming et al., 2006; Celik et al., 2008; Kaufmann et al., 2009). A central localisation of the substrate binding site is also in accordance with the alternate access hypothesis of transport, which implies that the substrate binding site has a central location from which the extracellular and intracellular environments alternately are accessible (see 1.3.1 SERT classification and function).

Recent studies have, however, also suggested that a second substrate binding site is located in the extracellular vestibule of the NSS transporters and that substrate binding in this site allosterically triggers intracellular release of Na^+ and substrate from the primary site (Shi et al., 2008; Shan et al., 2011; Zhao et al., 2011). However, another study concludes that LeuT has one high-affinity central substrate binding site and that transport follows a single-substrate kinetic mechanism (Piscitelli et al., 2010).

LeuT has been cocrystallised with clomipramine, imipramine and desipramine (TCA antidepressants) and sertraline, (*R*)- and (*S*)-fluoxetine (SSRI antidepressants) (Singh et al., 2007; Zhou et al., 2007; Zhou et al., 2009). In these crystal structures, the inhibitors, which are low-affinity LeuT binders, also bind in the extracellular vestibule of LeuT (Singh et al., 2007; Zhou et al., 2007; Zhou et al., 2009). The localisation of the extracellular vestibular binding site as the primary binding site of the SSRI and TCA drugs in SERT is, however, controversial as several studies indicate that these inhibitors interact with amino acids in the central binding site (Chen et al., 1997; Barker et al., 1998; Barker et al., 1999; Henry et al., 2006; Plenge et al., 2007; Walline et al., 2008; Andersen et al., 2009; Andersen et al., 2010; Sinning et al., 2010; Thompson et al., 2011). It has also recently been suggested that the tricyclic nucleus of the TCAs may be located in the extracellular vestibular region whereas the amine side chain points towards the substrate binding site (Sarker et al., 2010).

The existence of allosteric binding sites have been suggested in SERT as the dissociation of several drugs, e.g. imipramine, paroxetine, (*S*)-citalopram, sertraline, and fluoxetine, can be attenuated by other drugs (Plenge and Mellerup, 1985; Plenge et al., 1987; Plenge et al., 1990; Chen et al., 2005). The potency of (*S*)-citalopram for inhibiting 5-HT uptake is reduced by the Y95F (TM1), I172M (TM3) or the Y95F/I172M mutations, whereas the mutations do not affect the potency of paroxetine for inhibiting 5-HT transport. However, in µM concentrations, (*S*)-citalopram can attenuate the dissociation of [^{3}H]-paroxetine from wild type SERT as well as from the Y95F (TM1), I172M (TM3) and Y95F/I172M mutants, which hence indicates that there is an (*S*)-citalopram allosteric binding site that is distinct from the high-affinity binding site (Plenge et al., 2007).

1.4 Computer-based methods in structural biology and drug discovery

Most drugs on the market today were discovered either by chance observation or by systematic screening of a large numbers of natural and synthetic substances. These traditional

methods of drug discovery are now being supplemented by a more direct rational drug design, partly made possible by improved understanding of the biology of the disease process, and partly by knowledge about the 3D structure of drug target protein(s). Computer-based prediction of drug binding geometries and affinities through docking and scoring of compounds may complement the experimental binding analysis by adding molecular insight into the binding process.

1.4.1 Molecular mechanics

In computational chemistry, the classical molecular mechanics representation is most often used to model molecular systems. In classical molecular mechanics, the atomic structure of a molecule is not represented explicitly but is rather considered a collection of masses interacting with each other via harmonic forces where the different atoms of the molecules are represented as balls connected by springs (i.e., bonds) (Höltje et al., 2008).

1.4.1.1 Force fields

In molecular mechanics, the total energy of a molecule is calculated using terms of deviations from reference 'unstrained' bond lengths, angles and torsions as well as nonbonded interactions. Collections of such unstrained values together with empirically derived fit parameters (the force constants) are called force fields (Höltje et al., 2008). In general, force fields can be written as:

$$E_{tot} = E_{bonded} + E_{nonbonded}; \text{ or}$$

$$E_{tot} = (E_{bond} + E_{angle} + E_{dihedral}) + (E_{elec} + E_{vdw})$$

where E_{tot} is the total potential energy and the E_{bonded} and $E_{nonbonded}$ is the covalent and non-covalent bonding energy terms. The E_{bonded} term can be further subdivided into the E_{bond}, E_{angle} and $E_{dihedral}$, i.e., the bond stretching, angle bending, and torsional energy terms, respectively, and the $E_{nonbonded}$ term into the electrostatic and van der Waals (E_{elec} and E_{vdw}, respectively) energy terms (Höltje et al., 2008).

1.4.1.2 Energy minimisation, Monte Carlo and molecular dynamics methods

Conformational analysis of molecules using molecular mechanics may be performed using energy minimisation, Monte Carlo and molecular dynamics (MD) methods.

Drugs are assumed to interact with low-energy conformations of their targets, which is the conformation of molecules that is spontaneously obtained in nature. In computer-based methods, energy minimisation methods are used to obtain the favourable low-energy conformations of molecules. A commonly used energy minimisation method for larger systems is the conjugate-gradient method, where information is accumulated from one iteration to the next and is used to continually refine the direction of the minimisation towards the minimum (Höltje et al., 2008).

Monte Carlo is a conformational analysis method based on random (stochastic) searching (Höltje et al., 2008). An iteration of a Monte Carlo simulation consists of a random conformational move followed by energy minimisation of the new conformation and comparison with previously generated conformations. A conformation is only saved when it represents a unique, low-energy structure.

MD simulation methods aim to reproduce the time-dependent motional behaviour of molecules. At regular time intervals during the simulations, Newton's second law of motion is solved:

$$F_i(t) = m_i a_i(t)$$

F_i is the force on atom i at time t, m_i is the mass of atom i and a_i is the acceleration of atom i at time t. At time t, new positions and velocities of the atoms are calculated and the atoms are moved, hence generating a new conformation which is recorded in a trajectory. The procedure is repeated for a certain number of predefined time steps (Höltje et al., 2008).

1.4.2 Homology modelling

For many drugs, the 3D structure of the target they interact with to produce their biological effects is not known. In such cases, the homology modelling approach may be used to generate theoretical models of the protein targets.

The homology modelling approach takes advantage of the observation that 3D structure is a more conserved property during evolution than is the sequence of proteins belonging to the same family (Chothia and Lesk, 1986). The 3D structure of a known protein

(the ‘template’, e.g. LeuT) can hence be used to generate a theoretical model of a protein of unknown structure (the ‘target’, e.g. SERT) as long as the proteins are homologous, i.e., that they have evolved from a common ancestor. The conserved regions of a protein (the protein core) - for instance the 12 transmembrane spanning α-helices of the NSS transporters - are the regions where the sequence identity, and hence the structural similarity, between a template and a target is the highest and are the easiest to model. In contrast, the non-conserved regions, usually corresponding to the loop areas, may vary significantly in sequence as well as in length and are the most unreliable regions of a homology model.

The homology modelling approach consists of several distinct steps: (1) template identification, (2) amino acids sequence alignment, (3) model construction, and (4) refinement and evaluation of the model.

For many target structures, the template may already be known as only one or a few structures may have been solved by x-ray crystallisation. If, however, the template is unknown, a template structure must be identified by comparing the target sequence to all sequences of structurally known proteins in the protein data bank (PDB). The two major searching methods are FASTA (Pearson, 1990) and BLAST (Altschul et al., 1997).

Once a template has been identified, alignment of the target and template amino acids sequences is performed. Alignment of sequences may, however, not be straight-forward as the sequence identity between the two proteins in question may be very low and the sequences may vary in length. A multiple sequence alignment, where several homologous protein sequences are aligned, is thus always recommended in order to decrease the probability of incorrectly aligning amino acid sequences which again may result in incorrect homology models (Leach, 2001). Mistakes in the alignment step of the homology modelling process may result in the construction of incorrect homology models. Alignments should hence also be verified using experimental data if available. In some cases, sequence alignments of homologous proteins have been published, as for the NSS family (Beuming et al., 2006).

The construction of homology models consists of (1) generation of the amino acid backbone of structurally conserved regions, (2) construction of the non-conserved regions (loop modelling) and (3) placing of side chains. Loops are not always included in the models.

Following model construction, refinement of the homology model is often performed to remove close contacts between amino acids residues that have been added in the model

construction step and to relax high-energy structures. It may be performed using energy minimisation, Monte Carlo and/or molecular dynamics methods.

A very important step in the homology modelling procedure is the evaluation of the constructed models. The stereochemical properties of a model may be evaluated using the Structural analysis and verification server (SAVES; http://nihserver.mbi.ucla.edu/SAVES/) which contains computer programs that examine the quality of the 3D structure and report any significant deviations from the norm. In addition, evaluation of the model using experimental data (e.g. site-directed mutagenesis data, accessibility data) should be performed. Docking of known binders may also help evaluating the generated model.

The homology modelling approach was originally developed for soluble proteins, however, the approach can also be used for membrane protein modelling (Forrest et al., 2006). The accuracy of the constructed models depends on (1) the sequence identity between the template and target proteins, (2) the sequence alignment between the template and target, (3) the resolution at which the template protein crystal structure was solved. If an accurate alignment of the template and target sequences can be achieved, a sequence identity between the template and target structures of 50 % may yield models with C_α-RMSD of approximately 1 Å from the native structure in the transmembrane regions, whereas a C_α-RMSD of 2 Å may be obtained if the sequence identity between the template and target is approximately 30 % (Forrest et al., 2006).

1.4.3 Docking and scoring

Docking is a widely used method to predict the binding orientation of ligands in their macromolecular targets. In an ideal docking, both the ligand and receptor molecules are fully flexible. However, the degrees of freedom involved in such a docking makes it computationally unfeasible, and most docking programs today use a semi-flexible docking approach where the smaller ligands are flexible but the protein macromolecule is rigid (Leach, 2001). One approach to include some protein flexibility in the docking may also be to perform refinement of the protein side chains (and sometimes also the backbone) in the presence of the docked ligands, a method often called induced-fit docking (Sherman et al., 2006). Another method for incorporating protein flexibility in docking is by docking the ligands into several protein binding site conformations (ensemble docking). During ensemble docking, the

conformations may be experimental crystal structures, computationally generated structures (e.g. generated using Monte Carlo or MD methods), or consist of both.

Docking is often regarded to be successful when the root-mean-square-deviation (RMSD) between the predicted ligand orientation and the experimentally determined ligand orientation is ≤ 2 Å (Gohlke et al., 2000). In general, semi-flexible docking protocols have high success rates when a ligand is docked into its native crystal structure (self-docking). However, due to the structural rearrangements proteins undergo upon ligand binding, which may range from local movements of side chains to large domain movements, prediction of ligand orientation during docking of a ligand into a non-native structure (cross-docking) is more difficult and the success rates are significantly lower than in self-docking experiments. Protein flexibility in docking may hence be very important.

Scoring is used to describe the interaction between a protein and a ligand. Scoring functions may be used to rank the multiple orientations of one ligand in a binding site (pose ranking), or to predict the absolute binding affinity between a protein and a ligand and/or identify potential hits/leads for a given target by searching large ligand databases (virtual screening) (Huang et al., 2010). The free energy of binding (ΔG) is given by the Gibbs-Helmholtz equation:

$$\Delta G = \Delta H - T\Delta S = -RT \ln K_i$$

where ΔH is the enthalpy, T is the temperature (Kelvin), ΔS is the entropy, K_i is the binding constant and R is the gas constant (Höltje et al., 2008).

Four main scoring functions are available: the empirical, force-field, knowledge-based and consensus functions (Huang et al., 2010). The different functions differ significantly in accuracy and speed, and in general the most accurate scoring functions are the most time-consuming. Empirical scoring functions consist of weighted energy terms that describe known drug binding properties, e.g. hydrogen bonding, ionic, lipophilic and aromatic interactions and loss of ligand flexibility (entropy), whereas force-field scoring functions are based on the nonbonded interaction energy terms of molecular mechanical force fields (Huang et al., 2010). In comparison, knowledge-based scoring functions uses energy potentials derived from the structural information embedded in experimentally determined structures. Consensus scoring functions combine the empirical, knowledge- and force field-based functions (Huang et al., 2010). Due to their speed, the empirical scoring functions are the preferred scoring

functions for virtual screening of large databases. Training sets of protein–ligand complexes with known three-dimensional structures are, however, needed to generate empirical functions and scoring of ligands containing structural scaffolds not represented in the training set may be problematic (Huang et al., 2010).

1.4.4 Virtual screening

Virtual screening (VS) is a rapid *in silico* assessment of large compound libraries that is performed with the aim of detecting novel bioactive compounds. VS is performed using either structure-based or ligand-based methods, or a combination of the two. A comprehensive study of published VS papers show that more structure-based than ligand-based VS have been published so far (322 vs. 107 papers, respectively) (Ripphausen et al., 2010).

Structure-based VS is performed predominantly by docking. Of the 322 structure-based virtual screening papers identified, 215 contained docking into x-ray crystal structures and 73 into homology models (Ripphausen et al., 2010). In addition to docking, 'implicit' structure-based virtual screening methods are also available; for instance may structure- or structure-docking-based pharmacophore models be used for screening (Ripphausen et al., 2010). A pharmacophore model is 'the ensemble of steric and electronic features necessary to ensure the optimal supramolecular interactions with specific biologic target structure and to trigger (or to block) its biologic response' (Wermuth, 1998). Ligand-based VS is often performed using ligand-based 3D pharmacophore models generated by superimposing a set of active molecules (reference ligands) and determining ligand conformations that can be overlaid in such a way that a maximum number of important chemical features geometrically overlap (Wolber, 2008). Ligand-based VS screening may also be performed using 2D methods, for instance using fingerprint similarity searching methods.

Pharmacophore model generation involves conformational sampling of the ligands and alignment of the multiple generated conformations to determine their common chemical features and construct the pharmacophore models (Yang, 2010). The ligand sampling may be performed using either pre-enumeration or on-the-fly methods, i.e., either though precomputation of multiple ligand conformations or by performing ligand sampling during the pharmacophore modelling process. Alignment of the multiple conformations of the reference ligands may be performed using either point-based methods (superimposing pairs of

atoms, fragments or chemical features) or property-based methods (using molecular field descriptors, which are usually represented as sets of Gaussian functions) (Yang, 2010). The screening step in pharmacophore-based VS involves conformational sampling of the ligands in the database, and is performed using pre-enumeration or on-the-fly methods as for the sampling of the reference ligands during pharmacophore modelling step, and pharmacophore pattern identification (substructure searching), checking whether a pharmacophore pattern is present in a given ligand conformation (Yang, 2010).

Numerous commercial databases are available for virtual screening and the number of compounds included in the databases is increasing rapidly. Due to the large number of compounds available, screening of entire databases is computationally demanding and reduction of the number of compounds in a database through filtering is usually performed prior to screening. The best known filter may be the Lipinski 'rule of 5', which is a filter that predicts the 'druggability' of a compound. The rules predicts that poor absorption or permeation is more likely when a ligand has 1) more than 5 hydrogen bond donors or 2) more than 10 hydrogen acceptors, 3) the molecular weight (MW) is greater than 500 and 4) the calculated Log P (octanol-water partition coefficient, ClogP) is greater than 5 (Lipinski et al., 2001). The term 'rule of 5' hence reflects that the cutoffs for each of the four parameters are 5 or a multiple of 5. Multiple other filters may also be used, for instance absorption-distribution-metabolism-excretion-toxicity (ADME/Tox) filters. Virtual screening protocols that incorporate filtering are named multi-step protocols (Yang, 2010).

2. AIM OF STUDY

The serotonin transporter has a pivotal role in the central nervous system. By removing 5-HT from the synaptic cleft, the transporter plays a major role in the termination of serotonergic neurotransmission. Moreover, numerous therapeutic and illicit drugs also interact with the transporter. Knowledge about the 3D structure of SERT is of vital importance in order to understand how substrate transport in SERT occurs and how antidepressants and psychostimulant drugs such as cocaine prevent this transport. Such knowledge may be used for the development of new SERT inhibitors. Currently, however, no experimentally determined 3D structure of any eukaryotic NSS transporter has been solved by x-ray crystallisation. Instead, theoretical 3D homology models of SERT based on experimentally determined 3D structures of a prokaryotic homologous leucine transporter are used to study SERT.

The aim of the present study was to gain insight into the structure, function and ligand interactions in SERT using computational methods. The sub-goals were to:

a) construct homology models of SERT in occluded and outward-facing conformations
b) study the molecular mechanisms of substrate transport and inhibitor binding by performing molecular dynamics simulations of SERT-5-HT and SERT-(*S*)-citalopram complexes
c) study SERT-inhibitor interactions by flexibly docking of known inhibitors from several classes of drugs
d) perform virtual screening of three commercial databases to discover new SERT inhibitors
e) study the interactions of a series of potential antidepressants, 6-nitroquipazine alkyl analogues, by flexible docking

3. METHODS

In the present section, the methods used in the current work are described.

3.1 Software

Homology modelling and docking was performed using ICM software version 3.5 (www.molsoft.com). In paper 1, the POPC lipid bilayers were generated using the CHARMM-GUI membrane builder module (www.charmm-gui.org) and the MD simulations were performed using NAMD molecular dynamics simulator versions 2.6 and 2.7b1 (Phillips et al., 2005. The VMD molecular dynamics viewer version 1.8.6 was used to analyse the MD simulations and to generate average structures (Humphrey et al., 1996). The NAMD and VMD programs have been developed by the Theoretical and Computational Biophysics Group in the Beckman Institute for Advanced Science and Technology at the University of Illinois at Urbana-Champaign (Phillips et al., 2005) and are available at http://www.ks.uiuc.edu/Development/. In paper 3, the Instant JChem, GenerateMD and ScreenMD (JChem command line tools) of ChemAxon (www.chemaxon.com) were used for database management and 2D similarity searching, the Schrödinger software module QikProp (www.schrodinger.com) was used for calculation of the ADME/Tox descriptors and the Catalyst module of Accelrys Discovery studio 2.5 (www.accelrys.com) was used for generation of the 3D pharmacophore models and for screening of the Enamine, ChemBridge and ChemDiv databases.

3.2 Homology modelling

The comprehensive alignment of prokaryotic and eukaryotic NSS family members (Beuming et al., 2006) was used to adjust the alignment of the LeuT and SERT amino acids sequences generated by ICM. To generate homology models, ICM uses a rigid body homology modelling method where the target is constructed by transferring the backbone conformation of the core regions from the template to the target. The non-conserved loop regions are constructed through PDB loop searching by matching the loop regions in regard to sequence similarity and steric interactions with the surroundings of the model. The side chains of the identic amino acids are transferred directly from the template, while the side chains of non-conserved amino acids are either modelled (conservative change in amino acids) or are

added to the target without reference to the template (non-conservative change in amino acids), using the most probable rotamer of the side chains (Abagyan, 1994).

The ICM refineModel macro was used to energy optimise the constructed models (Abagyan and Totrov, 1994). The macro performs 1) side chain sampling using the program module Montecarlo-fast, 2) iterative annealing with tethers (harmonic restrains that pull an atom in the model to a static point represented by a corresponding atom in the template) and 3) a second side chain sampling. Iterations of Montecarlo-fast consist of a random move followed by local energy minimisation of a subset of the side chains and each iteration is accepted or rejected based on the energy. Selection of side chains for minimisation is based on the energy-gradient generated during the random move, and side chains above the energy gradient threshold are minimised. These side chains usually belong to the residues that are not conserved between the template and target structures and their neighbouring residues.

3.3 ICM PocketFinder

The ICM PocketFinder macro was used to detect possible binding pockets in the SERT 3D structures. The algorithm is based on a transformation of the Lennard-Jones potential calculated from the 3D protein structure and does not require any knowledge about potential ligands (An et al., 2005).

3.4 Docking

3.4.1 Semi-flexible docking

Binding pose prediction in ICM is performed using a Monte Carlo global optimisation procedure (Abagyan, 1994). In order to speed up the global optimisation procedure, the protein is included as a set of rigid pre-calculated grid potential maps representing van der Waals, hydrogen-bonding, electrostatic and hydrophobic ligand-receptor interaction terms. The energy function that is optimised during docking is then the internal conformational energy of the ligand (the ligand internal strain) based on the Empirical Conformational Energy program for Peptides (ECEPP)/3 molecular mechanics force field (Nemethy, 1992) and a weighted sum of the grid map values in ligand atom centres (Abagyan and Kufareva, 2009).

The global optimisation procedure begins by generation of a diverse set of ligand conformations *in vacuo* through sampling of the rotational and torsional degrees of freedom (Abagyan, 1994). The generated conformations are placed into the binding pocket are used as starting points for global optimisation of the energy function. Iterations of the global optimisation procedure consist of a random move of two types, either torsional, i.e., complete randomisation of a single arbitrarily chosen torsion angle, or positional, i.e., a pseudo-Brownian random translation and rotation of the ligand. The random move is followed by a local energy minimisation using an analytical gradient minimiser and the ligand conformation is either accepted or rejected based on the energy (Bursulaya et al., 2003). During the global optimisation procedure, a stack of low energy conformations is saved and ranked using the docking energy (see 3.6.1 Docking energy).

3.4.2 Flexible docking

Whereas a semi-flexible docking protocol was used in paper 1, a flexible docking protocol was used in papers 2-4. The protocol consisted of three distinct steps: (1) detection of a ligand binding pocket using ICM PocketFinder (An et al., 2005), (2) torsional sampling of the side chains of the amino acids constituting the binding pocket using biased probability Monte Carlo (BPMC) (Abagyan and Totrov, 1994) and (3) 4D flexible ligand docking (Bottegoni et al., 2009).

Torsional sampling of the protein side chains took place in the presence of a repulsive density representing a *generic* ligand. To calculate this repulsive density, the side chains of the amino acids in the selected pocket (except the alanine, glycine and cysteine amino acids) were simultaneously converted to alanine and an atom density grid map was generated for the "shaved" protein (Abagyan and Kufareva, 2009). During the 4D docking step, 3D receptor potential grid maps were generated for all the 47 binding pocket conformations generated during BPMC sampling and stored as a single data structure, the 4D grid. In the 4D grid, the first three dimensions represent regular Cartesian coordinates of the grid sampling nodes, whereas the fourth dimension represents an index of the pocket conformations (Abagyan and Kufareva, 2009). During Monte Carlo sampling, the ligand is allowed to change from the fourth coordinate via a special type of random move alongside the regular Cartesian translations and rotations. Because the receptor conformations are changed concurrently with the ligand conformations, a 4D simulation convergence time is comparable with that of a

single receptor docking – significantly shorter than an ensemble docking (Bottegoni et al., 2009).

3.5 Refinement

In paper 4, the refinement option in ICM was used to optimise two SERT-ligand complexes. During the refinement, the ligands were tethered to their original docking positions while the side chains of the amino acids surrounding the two selected ligands were sampled using BPMC (Abagyan and Totrov, 1994).

3.6 Scoring

Scoring is used to a) rank ligand conformations/orientations (pose ranking), b) predict the absolute binding affinity between the protein and ligand and/or c) identify potential hits/leads for a given target by searching large ligand databases (virtual screening).

3.6.1 Docking energy

The ICM docking energy function consists of the ligand internal energy and the intermolecular energy based on the grid maps used in the docking step. The docking energy is used to rank the different poses of a ligand obtained during docking rather than comparing the binding affinities of different ligands and does hence not account for the ligand entropy loss (decrease of conformational freedom upon binding).

3.6.2 Binding energy

In paper 1, the binding energy was calculated using the ICM calcBindingEnergy macro. The macro evaluates the binding energy using electrostatic, hydrophobic and entropic energy terms. The parameters for this macro were derived by (Schapira et al., 1999).

3.6.3 VLS score

In papers 2-4, the empirical ICM virtual ligand screening (VLS) scoring function was used to compare the binding energies of different ligands. In order to calculate the score, the scoring function uses steric, entropic, hydrogen bonding, hydrophobic, and electrostatic terms

and also includes a correction term that is proportional to the number of atoms in the ligand to avoid the bias toward larger ligands (Schapira et al., 2003).

3.7 Molecular dynamics simulations

Molecular dynamics (MD) simulations are used to simulate the time-dependent motion of molecules. In paper 1, five MD simulations of SERT-ligand complexes embedded in lipid bilayers were performed.

3.7.1 Membrane

The automated CHARMM-GUI membrane builder module (Jo et al., 2007) was used for the generation of the palmitoyloleoylphosphatidylcholine (POPC) lipid bilayers around the five SERT-(ligand) complexes. The membrane builder module is divided into 5 steps: 1) uploading of PDB structure, 2) protein orientation, 3) system size determination, 4) generation of lipid, ion, and water components, and 5) assembly of the components generate during the previous step.

The pre-orientated LeuT structure (Yamashita et al., 2005) from the Orientations of Proteins in Membranes (OPM) database (Lomize et al., 2006) was used to orient the SERT model in the membrane by superimposing the LeuT and SERT. The replacement method, in which SERT was packed with lipid-like spheres whose positions were used to place randomly chosen POPC lipid molecules from a lipid library composed of 2000 different lipid conformations of lipids generated by MD simulations of pure lipid bilayers (Jo et al., 2007), was used to generate the membrane. A total of 115 lipids were included in the outer bilayer and 121 in the inner bilayer and TIP3 water molecules and K^+ and Cl^- ions were added to fully solvate the system. The system size measured approximately 100x100x100 Å in the x, y and z directions.

3.7.2 CHARMM force fields

Equilibration of the generated SERT-(ligand)-membrane complexes and the longer MD simulations were performed using CHARMM force fields. The CHARMM22/CMAP protein force field (Mackerell et al., 1998; Mackerell et al., 2004), CHARMM27 lipid force field (Feller and Mackerell, 2000; Feller et al., 2002) and CHARMM36 force field for ligands (Vanommeslaeghe et al., 2010) were used.

During the simulations, Nosé–Hoover–Langevin dynamics were used to simulate the NPT ensemble, in which the number of atoms (N), the pressure (P) and temperature (T) are fixed. This method combines the Nosé–Hoover constant pressure method with piston fluctuation control implemented using Langevin dynamics by coupling the piston to a heat bath. During the simulations, a flexible cell was used, allowing the height, length, and width of the cell to fluctuate independently during the simulation, which is very useful for anisotropic systems such as membranes.

3.8 Virtual screening

In paper 3, virtual screening of the Enamine, ChemBridge and ChemDiv databases was performed. The multi-step combined virtual screening protocol is outlined in Figure 2.

FILTERING

Prefiltering using Lipinski ‘rule of 5’ and Veber filters

2D fingerprint-based screening

Physicochemical property filter

ADME/Tox filter

↓

LIGAND-BASED SCREENING

3D pharmacophore-based screening

↓

STRUCTURE-BASED SCREENING

Flexible docking

Visual inspection

↓

BIOLOGICAL EVALUATION

Radioligand competition binding assays

Figure 2. The multi-step combined virtual screening protocol.

3.8.1 Filtering of databases

The Lipinski ‘rule of 5’ (Lipinski et al., 2001) and the Veber filters (Veber et al., 2002) were used to obtain drug-like compounds. 2D similarity searching was performed using the ChemAxon software. The pharmacophore-based structural (chemical hashed) fingerprints were constructed using the GenerateMD command line tool, whereas the metrics optimisation and the 2D similarity searching was performed using the ScreenMD command line tool of ChemAxon. Physicochemical and ADME/Tox filters were also included in the protocol to ensure that all ligands contained positively ionisable moieties and to remove ligands with unfavourable ADME/Tox profiles.

3.8.2 3D ligand-based screening

The HypoGen module of Catalyst was used to generate the 3D pharmacophore models. HypoGen uses a pre-enumeration method to sample ligand conformations. The FAST algorithm was used to perform conformational sampling of ligands. The pharmacophore models were constructed by feature-based molecular alignment of the ligands to determine the essential common chemical features. The HipHop algorithm (Barnum, 1996) of Catalyst was used for pharmacophore pattern identification. The algorithm identifies common features by a pruned exhaustive search, starting by finding all two-feature models and expands the model until no more configurations can be found. Each conformation is then scored based on the degree to which it is common to the input and its estimated rarity (Barnum, 1996). During pharmacophore mapping, the compounds were allowed to deviate from the pharmacophore models with maximum one feature (except positively ionisable (PI) group) in order to pass the screening.

3.8.3 Structure-based screening

The flexible docking protocol was used to dock the ligands in SERT (3.4.2 Flexible docking and 3.5.3 VLS scoring). The ligands were docked into 47 binding pocket conformations of the outward-facing SERT homology model constructed using the LeuT 3F3A x-ray crystal structure as template using the 4D docking approach (Bottegoni et al., 2009). The VLS scoring function was used to score the different ligands. The top-scored ligands were visually inspected and ligands that interacted with D98 (TM1) were selected for

biologic evaluation. A PubChem (http://pubchem.ncbi.nlm.nih.gov/) similarity search was also performed in order to avoid evaluating known SERT binders.

3.8.4 Biological evaluation

The biological evaluation of the purchased compounds was performed using rat neocortical tissue. The compounds were screened for their ability to inhibit the binding of [^{3}H]-citalopram and compounds that caused at least 60 % inhibition of [^{3}H]-citalopram binding were included in a detailed examination. The estimated log IC_{50} was used to obtain the K_i by applying the Cheng-Prusoff approximation (Cheng and Prusoff, 1973). The biological evaluation was performed by our cooperation partners in Krakow, Poland.

4. SUMMARY OF RESULTS

4.1 Paper 1

Substrate binding and translocation of the serotonin transporter studied by docking and molecular dynamics simulations

Journal of Molecular Modeling, 2011, DOI 10.1007/s00894-011-1133-1

An occluded SERT homology model based on the LeuT 2A65 template (Yamashita et al., 2005) was constructed and used for docking of 5-HT and ten tryptamine derivatives and the SSRI (*S*)-citalopram. The ligands were docked into the putative substrate binding site detected by ICM PocketFinder using a semiflexible docking approach, and two possible ligand binding orientations for each ligand were observed. Based on the docking results, two SERT-5-HT- and two SERT-(*S*)-citalopram complexes were selected for molecular dynamics simulations. The apo-SERT structure was also included in the MD simulation study.

Following the MD simulations, average structures based on the ten last nanoseconds of each of the five simulations were generated and ICM PocketFinder (An et al., 2005) was used to detect possible pockets in the structures. Interestingly, the results showed that the substrate binding pocket in the SERT-5-HT^{B} average structure had started to elongate towards the cytoplasmic region, whereas another pocket had started to form from the cytoplasm and up towards the elongated substrate binding pocket. Based on the MD results, we suggest that formation and breakage of ionic bonds between amino acids in TMs 6 and 8 and IL1 and their interaction partners may play a role in substrate translocation.

4.2 Paper 2

Molecular mechanism of serotonin transporter inhibition elucidated by a new flexible docking protocol

Submitted to *European Journal of Medicinal Chemistry, 2011*

An outward-facing SERT homology model based on the LeuT 3F3A template (Singh et al., 2008) was generated and 58 known SERT inhibitors were docked using a new flexible docking protocol. The new protocol consisted of (1) detection of a ligand binding pocket using ICM PocketFinder, (2) sampling of the side chains of the amino acids using biased probability Monte Carlo (BPMC) procedure (Abagyan and Totrov, 1994), and (3) 4D docking of the ligands (Bottegoni et al., 2009). The side chain sampling of the amino acids belonging

to the binding pocket resulted in the generation of 47 binding pocket conformations into which the known inhibitors were docked using the 4D docking procedure (Bottegoni et al., 2009). The flexible docking suggested that the ligands occupy the putative substrate binding site of SERT as well as the lower regions of the extracellular vestibule. Structure-docking-based pharmacophore models were also generated to illustrate the observed binding modes of the ligands in the four most populated binding pocket conformations.

4.3 Paper 3

Identification of novel serotonin transporter compounds by virtual screening and experimental verification

Manuscript, 2011

Virtual screening of the Enamine, ChemBridge and ChemDiv databases was performed using a multi-step combined protocol. The number of compounds to screen was reduced using several filters prior to the 3D ligand-based screening step. Ten 3D pharmacophore models generated based on the 58 known SERT inhibitors (paper 2) were used in this step. The 3D pharmacophore-based screening step was followed by flexible docking of the identified compounds. The 47 binding pocket conformations that had been generated through side chain sampling and used for docking of the known inhibitors (paper 2) were used in the 4D docking procedure (Bottegoni et al., 2009). The compounds to purchase and biologically evaluate through radioligand competition binding studies were selected by visual inspection of the docking results. In total, 182 compounds were purchased and biologically evaluated *in vitro* using radioligand binding studies and 37 novel SERT inhibitors were identified. Several of the identified binders had nM SERT binding affinities.

4.4 Paper 4

Synthesis, docking and antidepressant evaluation of long-chain alkylnitroquipazines, inhibitors of the serotonin transporter

Manuscript, 2011

Twelve alkyl analogues (**1-12**) of the highly selective and potent SERT inhibitor 6-nitroquipazine (6-NQ) were synthesised and the SERT binding affinities were determined. In order to explain the varying affinities of the analogues, the compounds were docked into the outward-facing and occluded SERT homology models using the NMR structure of the octyl analogue (**8**) solved in the present study to construct the ligands. The docking results showed that the outward-facing SERT model best accommodated the compounds and indicated that the analogues interact with SERT in an orientation where their 6-nitro-quinolone moieties are located near extracellular loop 4 (EL4) in the extracellular regions of the transporter whereas the ligand alkyl side chains are located in the hydrophobic lower regions of the transporter. In this orientation, the protonated amine moiety of the analogues was in the vicinity of D98 (TM1). The antidepressant activities of the analogues with the highest affinities, **8-12**, were also evaluated using the *in vivo* forced swim and locomotor tests. The tests suggested that **8**, **10** and **12** have weak antidepressant activity.

5. DISCUSSION

The serotonin transporter (SERT) is one of the most studied drug targets in the CNS. Several drugs interact with the transporter, including the TCA and SSRI antidepressants and psychostimulants such as cocaine and amphetamines. The exact 3D structure of SERT is, however, not known and in the present study, SERT homology models were thus constructed in order to study the structure and function of the transporter.

5.1 LeuT as a template for homology modelling of SERT

Two theoretical SERT homology models were constructed based on x-ray crystal structures of the prokaryotic homologous leucine transporter (LeuT) (Yamashita et al., 2005; Singh et al., 2008). The homology models represent occluded and outward-facing SERT conformations.

Though the overall sequence identity between LeuT and SERT is as low as 21%, the substrate binding and extracellular vestibular regions detected by ICM PocketFinder have higher sequence identity and similarity (approximately 40 % identity and 60 % similarity) (Table 1). One major difference between the two transporters is the substitution of G24 in LeuT to D98 in SERT (corresponding to D79 and D75 in DAT and NET, respectively). In the LeuT crystal structures, the leucine carboxylate coordinates the Na1 sodium ion and it has been proposed that the aspartic acid in the monoamine transporters replaces the leucine carboxylate, complementing the difference between the amino acid and monoamine transporters (Yamashita et al., 2005).

All in all, LeuT is considered to be a good template for modelling of SERT. However, the homology modelling approach in general has its weaknesses and errors e.g. in the crystal structure template or in the alignment between the template and target sequences may have profound impacts on the generated models. The sequence identity between the template and target structures is also an important factor, and though some regions may be relatively conserved between the template and target structures and hence may be used to construct a probable structure of the target protein, other regions may be more uncertain. TMs 4 and 12 are for instance less conserved between LeuT and SERT than are the TMs involved in substrate binding (Beuming et al., 2006). Considerable differences between LeuT and SERT

also exist in certain loop regions, especially in EL2, where SERT contains a large insert not present in LeuT (Beuming et al., 2006). One of the loops, EL4, is located in the outer regions of the binding pocket detected in the outward-facing SERT homology model and hence also in the extracellular vestibular pocket detected in the occluded homology models, and may be of importance in ligand binding in this region of SERT. A comparison of the LeuT, SERT, DAT and NET amino acids in the binding pockets detected in the occluded and outward-facing SERT homology models is presented in Table 1.

5.2 Molecular mechanism of substrate translocation

The docking of 5-HT into the putative substrate binding site of SERT (paper 1) resulted in the identification of two possible binding modes of 5-HT in SERT. In both binding modes, the amine moiety of 5-HT formed a salt bridge with D98 (TM1) and the C6 position of the indole ring was oriented towards A173. The differences between the two binding modes was the orientation of the C5 position of the indole ring, which in the SERT-5-HT^{A} binding mode was pointing in the direction of Y176 (TM3), S438 and T439 (TM8) and in the direction of A169 (TM3) and F341 (TM6) in the SERT-5-HT^{B} binding mode. Very similar 5-HT binding modes have also been found by two other groups (Celik et al., 2008; Kaufmann et al., 2009). Similarly, two possible (*S*)-citalopram binding modes were also detected by docking of the inhibitor into the putative substrate binding pocket in occluded homology model. In both binding modes the amine moiety of the inhibitor was located in the vicinity of D98 (TM1) and the cyanophtalane moiety in the hydrophobic region of the binding pocket (near A169, A173 (TM3), V343 (TM6) and G442 (TM8). The localisation of the fluorophenyl moiety of (S)-citalopram, however, differed in the two binding modes: in the SERT-(*S*)-citalopram^{A} binding mode this moiety was pointing towards F335 (TM6), whereas it in the SERT-(*S*)-citalopram^{B} binding mode this moiety was juxtaposed between Y95 (TM1) and S438 (TM8). The docking results of (*S*)-citalopram clearly showed that the putative substrate binding detected in the occluded SERT homology model was small for the large (*S*)-citalopram inhibitor.

Table 1. Comparison of amino acids in LeuT and SERT, DAT and NET based on the comprehensive alignment of NSS transporters (Beuming et al., 2006). a) Amino acids in the putative SERT substrate binding site, b) Additional amino acids in the extracellular vestibular region. Red amino acids: non-conserved amino acids between the transporters.

	LeuT	SERT	DAT	NET	Location
a)	N21	Y95	F76	F72	
	G24	D98	D79	D75	TM1
	G26	G100	A81	A77	
	P101	A169	S149	A145	
	V104	I172	V152	V148	TM3
	A105	A173	G153	G149	
	Y108	Y176	Y156	Y152	
	F253	F335	F320	F317	
	T254	S336	S321	S318	
	S259	G338	G323	G320	TM6
	F259	F341	F326	F323	
	A261	V343	V328	V325	
	S355	S438	S422	S419	
	S356	T439	A423	S420	TM8
	A358	A441	G425	G422	
	I359	G442	G426	G423	
b)	L25	L99	L80	L76	
	G26	G100	A81	A77	TM1
	R30	R104	R85	R81	
	V33	Y107	Y88	Y84	
	Y107	Y175	F155	Y151	TM3
	I111	I179	I159	II55	
	L255	L337	L322	L319	TM6
	G318	A398	A383	A380	
	-	K399	K384	T381	
	-	D400	D385	E382	
	-	A401	-	-	
	A319	G402	G386	G383	EL4
	F320	P403	P387	A384	
	L322	L405	L389	L386	
	G323	L406	I390	V387	
	F324	F407	F391	F388	
	D401	K490	T473	T470	
	D404	E493	D476	D473	TM10
	G408	T497	A480	A477	

(*S*)-citalopram was also docked into the binding pocket detected in the outward-facing SERT homology model using a flexible docking approach (paper 2). The latter binding pocket better accommodated the inhibitor and the results of docking into this pocket suggested that the cyanophtalane moiety of (*S*)-citalopram may protrude out of the putative substrate binding

pocket and interact with amino acids in the lower parts of the extracellular vestibule, while the fluorophenyl moiety may interact in the hydrophobic region of the putative substrate binding site.

X-ray crystal structures are rigid snapshots of the most stable conformation of a protein. However, SERT and other NSS transporters are flexible proteins and the LeuT crystal structures, which are occluded or outward-facing, do not reveal much about how substrates are transported. Thus, in paper 1, MD simulations of SERT in complex with its substrate 5-HT and the SSRI (*S*)-citalopram were performed in order to study conformational changes that may take place upon substrate and inhibitor binding.

Interestingly, we observed that the substrate binding pocket of one of the two SERT-5-HT complexes, the SERT-5-HT^{B} complex, started to elongate towards the cytoplasm during the MD simulation. Simultaneously, a vestibule stretching from the cytoplasm towards the elongated substrate binding pocket began to emerge. Our results suggest that the rearrangement of TMs 6 and 8 as well as IL1 may result in opening of a permeation pathway leading from the substrate binding site to the cytoplasm. Furthermore, the extracellular vestibular pockets that were detected by ICM PocketFinder in the initial SERT model could not be detected in the SERT-5-HT^{B} average structure, indicating that while the cytoplasmic pathway started to open, the extracellular pathway closed.

A mechanism for transport in SERT and the other NSS transporters has been proposed by Forrest el al. (Forrest et al., 2008). By extensively mutating amino acids predicted to be buried in the cytoplasmic region of SERT to cysteine and measuring the reactivity of the cysteine residues, they show that many of the amino acids predicted to be buried in fact were accessible to reagents from the cytoplasmic side of the membrane. The accessibility changes were detected according to which ligand was tested: 5-HT and ibogaine, an inhibitor that presumably stabilises SERT in an inward-facing conformation (Jacobs et al., 2007), increased the reactivity of several of the inserted cysteines, whereas almost all positions in this pathway were less accessible in the presence of cocaine, which most likely stabilises an outward-facing conformation of SERT (Zhang and Rudnick, 2006; Forrest et al., 2008; Tavoulari et al., 2009; Torres-Altoro et al., 2010). The accessibility data suggested that amino acids from TMs 1, 5, 6 and 8 contribute to the cytoplasmic permeation pathway (Forrest et al., 2008). These TMs have also been suggested to form the cytoplasmic permeation pathway in DAT (Shan et al., 2011).

Though our results indicate that a conformational change in SERT from an occluded to an inward-facing conformation had started to take place during the MD simulation of the SERT-5-HT^{B} complex, the MD simulations performed were relatively short. The prolongation of the SERT-5-HT^{B} simulation to 49 ns indicated that the structure had stabilised, however, no major conformational changes occurred during the prolongation and hence indicates that the simulation length should be further increased. Due to the short simulation times, no major helical conformational changes were observed and a direct role of TMs 1 and 5 in formation of a cytoplasmic permeation pathway hence cannot be observed in our models. However, our results indicate that further movement of TMs 6 and 8 may result in relocation of TMs 1 and 5, making the cysteine mutants in the helices more solvent accessible.

5.3 Binding of inhibitors

In papers 2-4, the ligands were docked into an outward-facing SERT homology model using a flexible docking protocol. This homology model was used as studies indicate that SERT inhibitors may interact with SERT in an outward-facing conformation (Zhang and Rudnick, 2006; Forrest et al., 2008; Tavoulari et al., 2009; Torres-Altoro et al., 2010). The binding pocket detected in the outward-facing model was also significantly larger than the binding pockets detected in the occluded model and was hence believed to better accommodate the SERT inhibitors, which in general are larger compounds than the substrates.

SERT flexibility was furthermore taken into consideration when docking in the outward-facing model of SERT. Torsional sampling of the binding pocket amino acid side chains resulted in the generation of 47 binding pocket conformations into which the ligands were docked using the 4D docking approach (Bottegoni et al., 2009). Including protein flexibility in docking is known to be important in order to obtain as good docking results as possible (Abagyan and Kufareva, 2009). Importantly, there are also indications that inhibitors interacting with the transporter may stabilise different SERT conformations (Tavoulari et al., 2009).

The side chain torsional sampling of the amino acids in the binding pocket detected in the outward-facing SERT model indicated that the extracellular gate in this model was not fully opened. Interestingly, docking of the known SERT inhibitors (paper 2) and the docking of the ligands during the virtual screening (paper 3) indicated that the ligands preferred a

conformation where the distance between the Y176 (TM1) and F335 (TM6), the aromatic amino acids of the extracellular gate, was approximately twice that of the outward-facing model, i.e., 8.7 Å in binding pocket conformation 24 vs. 4.4 Å in the initial outward-facing homology model. The equivalent distance in the occluded homology model was 2.3 Å. The results of the evaluation docking performed in paper 2 also showed that the initial outward-facing homology model could not accommodate the majority of the ligands.

Amino acids that are located in the putative substrate binding pocket and extracellular vestibular region of SERT and that have been found to affect inhibitor binding in site-directed mutagenesis studies are shown in Figure 3. The flexible docking of the ligands in papers 2 showed that the ligands occupied a region corresponding to the putative central substrate binding site and the lower parts of the extracellular vestibule. Though no docking restraints were used, the docking of the 58 known SERT inhibitors revealed that the amine moieties of the ligands interacted with D98 (TM1), located in the putative substrate binding region of the pocket. In fact, of the 58 inhibitors docked, only four of the inhibitors did not interact with D98 (only the top-scored binding orientation of each ligand was evaluated). The docking results showed that the majority of the inhibitors also had an aromatic moiety located juxtaposed between the extracellular gating amino acids Y176 (TM1) and F335 (TM6) and a hydrophobic or aromatic moiety near A169, I172 and A173 (all TM1) and V343 (TM6). Furthermore, the halogen atoms of the inhibitors containing such moieties were in the majorities of cases located in the lower parts of the extracellular vestibule. Interestingly, the LeuT-SSRI crystal structures (PDB id 3GWU, 3GWV, 3GWW) reveal that the halogen atoms of sertraline and fluoxetine in LeuT are located in the same region of the transporter, in a region the authors name the halogen-binding pocket (HBP) (Zhou et al., 2009). The HBP consists of amino acids L99, G100, W103, R104 (TM1), Y176, I179 (TM3) and F335 (TM6) in SERT (Zhou et al., 2009). This region is highly conserved among LeuT and the monoamine transporters, and of the seven amino acids, only one differs between SERT and DAT/NET (an alanine in DAT and NET corresponds to G100 in SERT) and only one amino acid is non-conserved between LeuT and SERT (SERT W103/LeuT L29) (Table 1). Our docking results hence suggest that the HBP can be occupied even if the ligands bind in the central substrate binding pocket.

Analysis of the docking results from the 37 compounds that were identified in the virtual screening of the Enamine, ChemBridge and ChemDiv databases (paper 3) also showed that the compounds occupied the same regions of SERT as the known inhibitors (paper 2).

Docking of 6-nitroquipazine and the twelve alkyl analogues (paper 4) suggested that these ligands, which are quite different in structure from the ligands docked in papers 2 and 3, orient their 6-nitro-quinoline moiety in the extracellular region of the binding pocket near EL4 whereas the protonated piperazine nitrogen moiety may interact with D98 (TM1). Importantly, docking of 6-NQ and the twelve analogues revealed that including multiple SERT binding pocket conformations during the docking of very flexible ligands may not be optimal. The results also show that refining the binding pocket in the presence of a ligand may further improve the docking results. Refinement of the SERT-ligand complexes in paper 2 may also have been performed to improve the docking scores.

During the visual inspection of the virtual screening docking results (paper 3), the possible ionic interaction between the ligands and SERT was used as a criterion for selecting compounds to purchase and biologically evaluate. Several studies have suggested that D98 (TM1) plays a key role in substrate and inhibitor binding through formation of an ionic interaction with the protonated aminergic ligands (Barker et al., 1999; Celik et al., 2008; Andersen et al., 2010; Sinning et al., 2010). In addition to the effects mutation of D98 (TM1) has on inhibitors, there are several other studies that also indicate that inhibitors occupy the putative substrate binding site of SERT. The conservative S438T (TM8) mutation in the substrate binding site of SERT reduces the potency of several inhibitors to inhibit [^{3}H]-5-HT uptake and [^{3}H]-MADAM binding, including the SSRIs (*S*)-citalopram, paroxetine and sertraline, the TCAs amitriptyline, clomipramine and imipramine and the cocaine analogue RTI-55 (Andersen et al., 2009). Multiple studies also indicate that mutations of Y95 (TM1) and I172 (TM3) in the putative substrate binding site affect the potency of a wide range of inhibitors (Chen et al., 1997; Barker et al., 1998; Henry et al., 2006; Plenge et al., 2007; Walline et al., 2008; Andersen et al., 2010). Very recently, the importance of I172 for inhibitor binding was also shown *in vivo* using transgenic mice bearing the I172M mutation (Thompson et al., 2011). In the SERT M172 transgenic mice, 5-HT transport was not affected; however, the potency of multiple inhibitors to inhibit [^{3}H]-5-HT transport was significantly reduced, especially the potencies of fluoxetine, cocaine, citalopram and (*S*)-citalopram (Thompson et al., 2011). Studies also suggest that Y95, D98 (TM1), I172, N177 (TM3), F341 (TM6) and S438 (TM8) are key determinants for (*S*)-citalopram binding in SERT, whereas TCAs may form a salt bridge with D98 (TM1) and orient the tricyclic ring between A173 (TM3)/T439 (TM8) and F335 (TM6) (Andersen et al., 2010; Sinning et al., 2010).

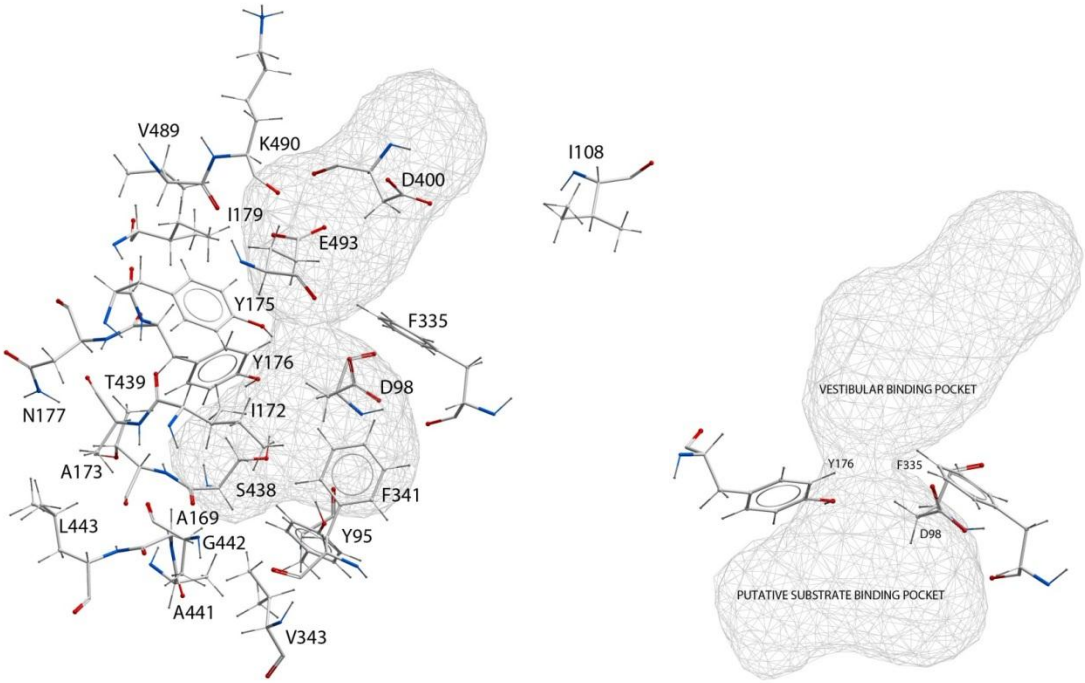

Figure 3. Localisation of amino acids suggested being involved in inhibitor binding in SERT. The references are given in the text.

However, LeuT has been crystallised with both TCAs (imipramine, desipramine and clomipramine) and SSRIs (sertraline, (*R*)-fluoxetine and (*S*)-fluoxetine), which are low-affinity LeuT inhibitors (Singh et al., 2007; Zhou et al., 2007; Zhou et al., 2009). The x-ray crystal structures show that the inhibitors are located in the extracellular vestibule, separated from the substrate binding site by the aromatic amino acids of the extracellular gate (Singh et al., 2007; Zhou et al., 2007; Zhou et al., 2009). Furthermore, the amine moieties of the ligands form a salt bridge with LeuT D401, or D404/Q34 in the case of (*R*)-fluoxetine/(*S*)-fluoxetine. In SERT, the corresponding amino acids to D401 and D404 in LeuT are K490 and E493 (TM10), respectively (Beuming et al., 2006). Mutations in the extracellular vestibular region of SERT have also been shown to affect the affinity of several SERT inhibitors. For instance, mutations of I179 (TM3) cause great reductions in the affinity of sertraline, whereas the K490T (TM10) mutation reduces the affinity of sertraline but improves the affinity of desipramine (Zhou et al., 2007; Zhou et al., 2009). The latter mutation also slightly though significantly reduces the affinity of (*S*)-citalopram, imipramine and clomipramine, as does mutations of D400 (EL4) (Andersen et al., 2009).

In the present work, docking of the ligands was performed into the large binding pocket of the outward-facing SERT homology model which consisted of both the putative

substrate binding site and the extracellular vestibular regions (papers 2-4) or into the putative substrate binding pocket in the occluded SERT model (paper 1). In addition, 6-nitroquipazine and the twelve alkyl analogues were docked into the extracellular vestibular binding pocket in the occluded SERT homology model (paper 4). The results, however, indicated that the pocket was too small to accommodate these ligands.

Due to the presence of the flexible EL4 loop (Mitchell et al., 2004; Yamashita et al., 2005; Singh et al., 2007; Zhou et al., 2007; Singh et al., 2008; Zhou et al., 2009), docking into the extracellular vestibular binding site is more uncertain than docking in the putative substrate binding site. In the flexible docking protocol presented, only side chain sampling was performed in order to generate the multiple binding pocket conformations, however, additional conformational sampling of the backbone of EL4 may be important when docking ligands in this region. The comprehensive alignment of prokaryotic and eukaryotic NSS transporters published by (Beuming et al., 2006) was used without any adjustments during the homology modelling process. It was, however, observed that superimposition of the LeuT TCA and SSRI crystal structures and the occluded SERT homology model based on the 2A65 LeuT crystal structure template (Yamashita et al., 2005) resulted in backbone collisions between EL4 of SERT and the cocrystallised TCA and SSRI ligands. By adjusting the alignment in the EL4 region, shifting the K399-D400-A401 region in SERT three steps to the left, the backbone collisions may have been avoided and docking of the ligands may have yielded better results.

5.4 Development of new SERT inhibitors

Virtual screening is a rapid and simple way of searching for novel inhibitors of SERT. There are multiple commercially available databases that can be screened, and the number of compounds is rapidly increasing. In paper 3, a multi-step combined virtual screening protocol was used to screen the Enamine, ChemBridge and ChemDiv databases. Due to the large number of compounds in the databases, different filters were used to reduce the number of compounds to screen. As we were looking for compounds with therapeutic potential, the Lipinski ‘rule of 5’ and Veber filters were used to obtain drug-like compounds. In total, approximately 2.5 million drug-like compounds were identified in the three databases downloaded in November 2009. The drug-like compounds were then filtered using 2D

fingerprint-based, physicochemical and ADME/Tox filters, further reducing the number of compounds to approximately 12.000.

The structures of the 58 known SERT inhibitors that were docked to SERT in paper 2 were used during the 2D similarity searching step and for generation of the 3D pharmacophore models. This large number of reference ligands and the diverse structures of the compounds were used to obtain as diverse compounds as possible. The ligand-based screening was followed by docking of the compounds into the 47 binding pocket conformations previously generated for docking of the reference ligands (paper 2) and visual inspection of the docking results and biological evaluation of the selected compounds was then performed. The evaluation of the compounds resulted in the identification of 37 SERT inhibitors.

Compared to other published SERT virtual screening protocols, the protocol used here is extensive. To our knowledge, only ligand-based virtual screening protocols using pharmacophore models have been published. In these studies, only a limited number of pharmacophore models were used for screening and fewer compounds were screened than in the present work (Wang et al., 2000; Enyedy et al., 2001; Enyedy et al., 2002; Enyedy et al., 2003; Macdougall and Griffith, 2008). The results of our study show that docking into SERT homology models can be included in – and be an important part of – virtual screening protocols. Our results furthermore show that protein flexibility may be included in docking of ligands during virtual screening.

However, it is important to keep in mind that selecting compounds for biological evaluation based on docking also may result in the loss of potential binders. Compounds may for instance be misdocked due to steric clashes with the protein, they may be docked correctly but score badly due to non-optimal ligand-protein contacts, they may be misdocked or score badly because water molecules or ions are not present, or they may be misdocked due to insufficient ligand sampling or docked correctly but scored incorrectly due to failures of the scoring function (Cavasotto and Abagyan, 2004).

Evaluating the success of the virtual screening protocol is of course difficult as the total number of SERT binders in the screening databases is unknown. The high number of identified SERT inhibitors and the high binding affinities of multiple of the compounds, however, suggest that the multi-step combined protocol was a good choice for virtual screening in order to detect SERT inhibitors. However, more inhibitors may possibly have

been detected if for instance the number of binding pocket conformations available for docking had been reduced or if more than one parallel docking was performed. Furthermore, though the docking results indicate that the identified compounds occupy the putative substrate binding site and the lower regions of the extracellular vestibule and form ionic interactions with D98 (TM1), other binding orientations cannot be ruled out as the compounds were not docked into for instance the extracellular vestibular site that corresponds to the LeuT TCA and SSRI binding site (Singh et al., 2007; Zhou et al., 2007; Zhou et al., 2009).

Using the multi-step combined virtual screening protocol, 37 compounds were identified as SERT binders. The next steps will be lead optimisation of the current results. Furthermore, due to the similarities between the three monoamine transporters (Table 1), prediction of the binding affinities of the compounds in DAT and NET also should be performed. The interaction of the compounds with other targets, e.g. 5-HT receptors, should also be determined.

6. Conclusion

In this thesis, two SERT homology models representing the occluded and outward-facing conformations of the transporter were constructed and used for docking of substrates and inhibitors, for studying the transport mechanism and in the virtual screening of three large commercial databases.

The MD simulations of the SERT-ligand complexes suggest that a rearrangement of TMs 6, 8 and IL1 may contribute in the opening of a cytoplasmic permeation pathway in SERT. Whereas docking into the putative substrate binding pocket in the occluded model suggested that the larger inhibitors could not be successfully docked due to their size, docking of inhibitors into the binding pocket detected in the outward-facing SERT model yielded better results. However, including SERT flexibility was important, as our results suggested that the extracellular gate (Y176, F335) was not fully opened. Docking of ligands into this pocket using the flexible docking approach, however, suggested that the inhibitors occupy parts of the putative substrate binding site and the extracellular vestibule. Flexible docking of ligand detected through virtual screening of three large databases also suggested that the outward-facing model can be used for virtual ligand screening. Using a multi-step combined virtual screening protocol, 182 compounds were biologically evaluated and 37 compounds were identified as SERT binders.

The work presented here may serve as basis for future studies of SERT structure and function. In the long term, novel SERT inhibitors with antidepressant properties may be developed based on hit compounds detected in this study. Furthermore, these methods may also be used on other proteins such as DAT and NET.

7. References

Abagyan R and Kufareva I (2009) The flexible pocketome engine for structural chemogenomics. *Methods Mol Biol* **575**:249-279.

Abagyan R and Totrov M (1994) Biased probability Monte Carlo conformational searches and electrostatic calculations for peptides and proteins. *J Mol Biol* **235**:983-1002.

Abagyan R, Totrov, M., Kuznetsov, D. (1994) ICM—A new method for protein modeling and design: Applications to docking and structure prediction from the distorted native conformation. *Journal of Computational Chemistry* **15**:488-506.

Altschul SF, Madden TL, Schaffer AA, Zhang J, Zhang Z, Miller W and Lipman DJ (1997) Gapped BLAST and PSI-BLAST: a new generation of protein database search programs. *Nucleic Acids Res* **25**:3389-3402.

An J, Totrov M and Abagyan R (2005) Pocketome via comprehensive identification and classification of ligand binding envelopes. *Mol Cell Proteomics* **4**:752-761.

Andersen J, Olsen L, Hansen KB, Taboureau O, Jorgensen FS, Jorgensen AM, Bang-Andersen B, Egebjerg J, Stromgaard K and Kristensen AS (2010) Mutational mapping and modeling of the binding site for (S)-citalopram in the human serotonin transporter. *J Biol Chem* **285**:2051-2063.

Andersen J, Taboureau O, Hansen KB, Olsen L, Egebjerg J, Stromgaard K and Kristensen AS (2009) Location of the antidepressant binding site in the serotonin transporter: importance of Ser-438 in recognition of citalopram and tricyclic antidepressants. *J Biol Chem* **284**:10276-10284.

Androutsellis-Theotokis A and Rudnick G (2002) Accessibility and conformational coupling in serotonin transporter predicted internal domains. *J Neurosci* **22**:8370-8378.

Barker EL, Moore KR, Rakhshan F and Blakely RD (1999) Transmembrane domain I contributes to the permeation pathway for serotonin and ions in the serotonin transporter. *J Neurosci* **19**:4705-4717.

Barker EL, Perlman MA, Adkins EM, Houlihan WJ, Pristupa ZB, Niznik HB and Blakely RD (1998) High affinity recognition of serotonin transporter antagonists defined by species-scanning mutagenesis. An aromatic residue in transmembrane domain I dictates species-selective recognition of citalopram and mazindol. *J Biol Chem* **273**:19459-19468.

Barnum D, Greene, J., Smellie, A., Sprague, P. (1996) Identification of common functional configurations among molecules. *J Chem Inf Comput Sci* **36**:563-571.

Beuming T, Shi L, Javitch JA and Weinstein H (2006) A comprehensive structure-based alignment of prokaryotic and eukaryotic neurotransmitter/Na+ symporters (NSS) aids in the use of the LeuT structure to probe NSS structure and function. *Mol Pharmacol* **70**:1630-1642.

Blakely RD, Berson HE, Fremeau RT, Jr., Caron MG, Peek MM, Prince HK and Bradley CC (1991) Cloning and expression of a functional serotonin transporter from rat brain. *Nature* **354**:66-70.

Bottegoni G, Kufareva I, Totrov M and Abagyan R (2009) Four-dimensional docking: a fast and accurate account of discrete receptor flexibility in ligand docking. *J Med Chem* **52**:397-406.

Bursulaya BD, Totrov M, Abagyan R and Brooks CL, 3rd (2003) Comparative study of several algorithms for flexible ligand docking. *J Comput Aided Mol Des* **17**:755-763.

Cavasotto CN and Abagyan RA (2004) Protein flexibility in ligand docking and virtual screening to protein kinases. *J Mol Biol* **337**:209-225.

Celik L, Sinning S, Severinsen K, Hansen CG, Moller MS, Bols M, Wiborg O and Schiott B (2008) Binding of serotonin to the human serotonin transporter. Molecular modeling and experimental validation. *J Am Chem Soc* **130**:3853-3865.

Chang AS, Starnes DM and Chang SM (1998) Possible existence of quaternary structure in the high-affinity serotonin transport complex. *Biochem Biophys Res Commun* **249**:416-421.

Chen F, Larsen MB, Sanchez C and Wiborg O (2005) The S-enantiomer of R,S-citalopram, increases inhibitor binding to the human serotonin transporter by an allosteric mechanism. Comparison with other serotonin transporter inhibitors. *Eur Neuropsychopharmacol* **15**:193-198.

Chen JG, Liu-Chen S and Rudnick G (1998a) Determination of external loop topology in the serotonin transporter by site-directed chemical labeling. *J Biol Chem* **273**:12675-12681.

Chen JG, Sachpatzidis A and Rudnick G (1997) The third transmembrane domain of the serotonin transporter contains residues associated with substrate and cocaine binding. *J Biol Chem* **272**:28321-28327.

Chen JX, Pan H, Rothman TP, Wade PR and Gershon MD (1998b) Guinea pig 5-HT transporter: cloning, expression, distribution, and function in intestinal sensory reception. *Am J Physiol* **275**:G433-448.

Chen NH, Reith ME and Quick MW (2004) Synaptic uptake and beyond: the sodium- and chloride-dependent neurotransmitter transporter family SLC6. *Pflugers Arch* **447**:519-531.

Cheng Y and Prusoff WH (1973) Relationship between the inhibition constant (K1) and the concentration of inhibitor which causes 50 per cent inhibition (I50) of an enzymatic reaction. *Biochem Pharmacol* **22**:3099-3108.

Chothia C and Lesk AM (1986) The relation between the divergence of sequence and structure in proteins. *Embo J* **5**:823-826.

Cool DR, Leibach FH and Ganapathy V (1990) Modulation of serotonin uptake kinetics by ions and ion gradients in human placental brush-border membrane vesicles. *Biochemistry* **29**:1818-1822.

Corey JL, Quick MW, Davidson N, Lester HA and Guastella J (1994) A cocaine-sensitive Drosophila serotonin transporter: cloning, expression, and electrophysiological characterization. *Proc Natl Acad Sci U S A* **91**:1188-1192.

Deisenhofer J, Epp O, Miki K, Huber R and Michel H (1985) Structure of the protein subunits in the photosynthetic reaction centre of Rhodopseudomonas viridis at 3Å resolution. *Nature* **318**:618-624.

Demchyshyn LL, Pristupa ZB, Sugamori KS, Barker EL, Blakely RD, Wolfgang WJ, Forte MA and Niznik HB (1994) Cloning, expression, and localization of a chloride-facilitated, cocaine-sensitive serotonin transporter from Drosophila melanogaster. *Proc Natl Acad Sci U S A* **91**:5158-5162.

Dubovsky SL and Warren C (2009) Agomelatine, a melatonin agonist with antidepressant properties. *Expert Opin Investig Drugs* **18**:1533-1540.

Enyedy IJ, Sakamuri S, Zaman WA, Johnson KM and Wang S (2003) Pharmacophore-based discovery of substituted pyridines as novel dopamine transporter inhibitors. *Bioorganic & medicinal chemistry letters* **13**:513-517.

Enyedy IJ, Wang J, Zaman WA, Johnson KM and Wang S (2002) Discovery of substituted 3,4-diphenyl-thiazoles as a novel class of monoamine transporter inhibitors through 3-D pharmacophore search using a new pharmacophore model derived from mazindol. *Bioorganic & medicinal chemistry letters* **12**:1775-1778.

Enyedy IJ, Zaman WA, Sakamuri S, Kozikowski AP, Johnson KM and Wang S (2001) Pharmacophore-based discovery of 3,4-disubstituted pyrrolidines as a novel class of monoamine transporter inhibitors. *Bioorganic & medicinal chemistry letters* **11**:1113-1118.

Eshleman AJ, Carmolli M, Cumbay M, Martens CR, Neve KA and Janowsky A (1999) Characteristics of drug interactions with recombinant biogenic amine transporters expressed in the same cell type. *J Pharmacol Exp Ther* **289**:877-885.

Feller SE, Gawrisch K and MacKerell AD, Jr. (2002) Polyunsaturated fatty acids in lipid bilayers: intrinsic and environmental contributions to their unique physical properties. *J Am Chem Soc* **124**:318-326.

Feller SE and Mackerell AD (2000) An Improved Empirical Potential Energy Function for Molecular Simulations of Phospholipids. *J Phys Chem B* **104**:7510-7515.

Fjorback AW, Pla P, Muller HK, Wiborg O, Saudou F and Nyengaard JR (2009) Serotonin transporter oligomerization documented in RN46A cells and neurons by sensitized acceptor emission FRET and fluorescence lifetime imaging microscopy. *Biochem Biophys Res Commun* **380**:724-728.

Forrest LR, Tang CL and Honig B (2006) On the accuracy of homology modeling and sequence alignment methods applied to membrane proteins. *Biophys J* **91**:508-517.

Forrest LR, Tavoulari S, Zhang YW, Rudnick G and Honig B (2007) Identification of a chloride ion binding site in Na+/Cl -dependent transporters. *Proc Natl Acad Sci U S A* **104**:12761-12766.

Forrest LR, Zhang YW, Jacobs MT, Gesmonde J, Xie L, Honig BH and Rudnick G (2008) Mechanism for alternating access in neurotransmitter transporters. *Proc Natl Acad Sci U S A* **105**:10338-10343.

Fuxe K, Dahlstrom A, Hoistad M, Marcellino D, Jansson A, Rivera A, Diaz-Cabiale Z, Jacobsen K, Tinner-Staines B, Hagman B, Leo G, Staines W, Guidolin D, Kehr J, Genedani S, Belluardo N and Agnati LF (2007) From the Golgi-Cajal mapping to the transmitter-based characterization of the neuronal networks leading to two modes of brain communication: wiring and volume transmission. *Brain Res Rev* **55**:17-54.

Gohlke H, Hendlich M and Klebe G (2000) Knowledge-based scoring function to predict protein-ligand interactions. *J Mol Biol* **295**:337-356.

Gu HH, Wall S and Rudnick G (1996) Ion coupling stoichiometry for the norepinephrine transporter in membrane vesicles from stably transfected cells. *J Biol Chem* **271**:6911-6916.

Henry LK, Field JR, Adkins EM, Parnas ML, Vaughan RA, Zou MF, Newman AH and Blakely RD (2006) Tyr-95 and Ile-172 in transmembrane segments 1 and 3 of human serotonin transporters interact to establish high affinity recognition of antidepressants. *J Biol Chem* **281**:2012-2023.

Huang SY, Grinter SZ and Zou X (2010) Scoring functions and their evaluation methods for protein-ligand docking: recent advances and future directions. *Phys Chem Chem Phys* **12**:12899-12908.

Humphrey W, Dalke A and Schulten K (1996) VMD: visual molecular dynamics. *J Mol Graph* **14**:33-38, 27-38.

Humphreys CJ, Wall SC and Rudnick G (1994) Ligand binding to the serotonin transporter: equilibria, kinetics, and ion dependence. *Biochemistry* **33**:9118-9125.

Höltje H-D, Sippl W, Rognan D and Folkers G (2008) *Molecular modeling. Basic priciples and applications. 3rd ed*. WILEY-VCH Verlag GmbH & Co KGaA.

Jacobs MT, Zhang YW, Campbell SD and Rudnick G (2007) Ibogaine, a noncompetitive inhibitor of serotonin transport, acts by stabilizing the cytoplasm-facing state of the transporter. *J Biol Chem* **282**:29441-29447.

Jardetzky O (1966) Simple allosteric model for membrane pumps. *Nature* **211**:969-970.

Jess U, Betz H and Schloss P (1996) The membrane-bound rat serotonin transporter, SERT1, is an oligomeric protein. *FEBS Lett* **394**:44-46.

Jo S, Kim T and Im W (2007) Automated builder and database of protein/membrane complexes for molecular dynamics simulations. *PLoS One* **2**:e880.

Just H, Sitte HH, Schmid JA, Freissmuth M and Kudlacek O (2004) Identification of an additional interaction domain in transmembrane domains 11 and 12 that supports oligomer formation in the human serotonin transporter. *J Biol Chem* **279**:6650-6657.

Kaufmann KW, Dawson ES, Henry LK, Field JR, Blakely RD and Meiler J (2009) Structural determinants of species-selective substrate recognition in human and Drosophila serotonin transporters revealed through computational docking studies. *Proteins* **74**:630-642.

Kendrew JC, Bodo G, Dintzis HM, Parrish RG, Wyckoff H and Phillips DC (1958) A three-dimensional model of the myoglobin molecule obtained by x-ray analysis. *Nature* **181**:662-666.

Kendrew JC, Dickerson RE, Strandberg BE, Hart RG, Davies DR, Phillips DC and Shore VC (1960) Structure of myoglobin: A three-dimensional Fourier synthesis at 2 A. resolution. *Nature* **185**:422-427.

Kilic F and Rudnick G (2000) Oligomerization of serotonin transporter and its functional consequences. *Proc Natl Acad Sci U S A* **97**:3106-3111.

Kocabas AM, Rudnick G and Kilic F (2003) Functional consequences of homo- but not hetero-oligomerization between transporters for the biogenic amine neurotransmitters. *J Neurochem* **85**:1513-1520.

Larsen MB, Elfving B and Wiborg O (2004) The chicken serotonin transporter discriminates between serotonin-selective reuptake inhibitors. A species-scanning mutagenesis study. *J Biol Chem* **279**:42147-42156.

Leach AR (2001) *Molecular modelling. Principles and applications. 2nd ed*. Pearson Education Limited.

Levine RR, Walsh CT and Schwartz-Bloom RD (2000) *Pharmacology. Drug actions and reactions 6th ed*. The Parthenon Publishing Group Limited.

Lipinski CA, Lombardo F, Dominy BW and Feeney PJ (2001) Experimental and computational approaches to estimate solubility and permeability in drug discovery and development settings. *Adv Drug Deliv Rev* **46**:3-26.

Lomize MA, Lomize AL, Pogozheva ID and Mosberg HI (2006) OPM: orientations of proteins in membranes database. *Bioinformatics* **22**:623-625.

Macdougall IJ and Griffith R (2008) Pharmacophore design and database searching for selective monoamine neurotransmitter transporter ligands. *J Mol Graph Model* **26**:1113-1124.

Mackerell AD, Bashford D, Bellott M, Dunbrack RL, Evanseck JD, Field MJ, Fischer S, Gao J, Guo H, Ha S, Joseph-McCarthy D, Kuchnir L, Kuczera K, Lau FTK, Mattos C, Michnick S, Ngo T, Nguyen DT, Prodhom B, Reiher WE, Roux B, Schlenkrich M, Smith JC, Stote R, Straub J, Watanabe M, Wiórkiewicz-Kuczera J, Yin D and Karplus M (1998) All-Atom Empirical Potential for Molecular Modeling and Dynamics Studies of Proteins. *Journal of Physical Chemistry B* **102**:3586-3616.

Mackerell AD, Jr., Feig M and Brooks CL, 3rd (2004) Extending the treatment of backbone energetics in protein force fields: limitations of gas-phase quantum mechanics in reproducing protein conformational distributions in molecular dynamics simulations. *Journal of computational chemistry* **25**:1400-1415.

Miller GM, Yatin SM, De La Garza R, 2nd, Goulet M and Madras BK (2001) Cloning of dopamine, norepinephrine and serotonin transporters from monkey brain: relevance to cocaine sensitivity. *Brain Res Mol Brain Res* **87**:124-143.

Mitchell SM, Lee E, Garcia ML and Stephan MM (2004) Structure and function of extracellular loop 4 of the serotonin transporter as revealed by cysteine-scanning mutagenesis. *J Biol Chem* **279**:24089-24099.

Mortensen OV, Kristensen AS, Rudnick G and Wiborg O (1999) Molecular cloning, expression and characterization of a bovine serotonin transporter. *Brain Res Mol Brain Res* **71**:120-126.

Murphy DL, Lerner A, Rudnick G and Lesch KP (2004) Serotonin transporter: gene, genetic disorders, and pharmacogenetics. *Mol Interv* **4**:109-123.

Nelson PJ and Rudnick G (1979) Coupling between platelet 5-hydroxytryptamine and potassium transport. *J Biol Chem* **254**:10084-10089.

Nemethy G, Gibson, K.D., Palmer, K.A., Yoon, C.N., Paterlini, G., Zagari, A., Rumsey, S., Scheraga, H. (1992) Energy parameters in polypeptides. 10. Improved geometrical parameters and nonbonded interactions for use in the ECEPP/3 algorithm, with application to proline-containing peptides. *Journal of Physical Chemistry* **96**:6472-6484.

Omori IM, Watanabe N, Nakagawa A, Cipriani A, Barbui C, McGuire H, Churchill R and Furukawa TA (2010) Fluvoxamine versus other anti-depressive agents for depression. *Cochrane Database Syst Rev*:CD006114.

Overington JP, Al-Lazikani B and Hopkins AL (2006) How many drug targets are there? *Nat Rev Drug Discov* **5**:993-996.

Owens MJ, Morgan WN, Plott SJ and Nemeroff CB (1997) Neurotransmitter receptor and transporter binding profile of antidepressants and their metabolites. *J Pharmacol Exp Ther* **283**:1305-1322.

Ozaslan D, Wang S, Ahmed BA, Kocabas AM, McCastlain JC, Bene A and Kilic F (2003) Glycosyl modification facilitates homo- and hetero-oligomerization of the serotonin transporter. A specific role for sialic acid residues. *J Biol Chem* **278**:43991-44000.

Patocka N and Ribeiro P (2007) Characterization of a serotonin transporter in the parasitic flatworm, Schistosoma mansoni: cloning, expression and functional analysis. *Mol Biochem Parasitol* **154**:125-133.

Pearson WR (1990) Rapid and sensitive sequence comparison with FASTP and FASTA. *Methods Enzymol* **183**:63-98.

Phillips JC, Braun R, Wang W, Gumbart J, Tajkhorshid E, Villa E, Chipot C, Skeel RD, Kale L and Schulten K (2005) Scalable molecular dynamics with NAMD. *Journal of computational chemistry* **26**:1781-1802.

Piscitelli CL, Krishnamurthy H and Gouaux E (2010) Neurotransmitter/sodium symporter orthologue LeuT has a single high-affinity substrate site. *Nature* **468**:1129-1132.

Plenge P, Gether U and Rasmussen SG (2007) Allosteric effects of R- and S-citalopram on the human 5-HT transporter: evidence for distinct high- and low-affinity binding sites. *Eur J Pharmacol* **567**:1-9.

Plenge P and Mellerup ET (1985) Antidepressive drugs can change the affinity of [3H]imipramine and [3H]paroxetine binding to platelet and neuronal membranes. *Eur J Pharmacol* **119**:1-8.

Plenge P, Mellerup ET, Honore T and Honore PL (1987) The activity of 25 paroxetine/femoxetine structure variants in various reactions, assumed to be important for the effect of antidepressants. *J Pharm Pharmacol* **39**:877-882.

Plenge P, Mellerup ET and Nielsen M (1990) Inhibitory and regulatory binding sites on the rat brain serotonin transporter: molecular weight of the [3H]paroxetine and [3H]citalopram binding proteins. *Eur J Pharmacol* **189**:129-134.

Quick M, Yano H, Goldberg NR, Duan L, Beuming T, Shi L, Weinstein H and Javitch JA (2006) State-dependent conformations of the translocation pathway in the tyrosine transporter Tyt1, a novel neurotransmitter:sodium symporter from Fusobacterium nucleatum. *J Biol Chem* **281**:26444-26454.

Ramamoorthy S, Bauman AL, Moore KR, Han H, Yang-Feng T, Chang AS, Ganapathy V and Blakely RD (1993) Antidepressant- and cocaine-sensitive human serotonin transporter: molecular cloning, expression, and chromosomal localization. *Proc Natl Acad Sci U S A* **90**:2542-2546.

Ripphausen P, Nisius B, Peltason L and Bajorath J (2010) Quo vadis, virtual screening? A comprehensive survey of prospective applications. *J Med Chem* **53**:8461-8467.

Rudnick G (1977) Active transport of 5-hydroxytryptamine by plasma membrane vesicles isolated from human blood platelets. *J Biol Chem* **252**:2170-2174.

Rudnick G (1998) Bioenergetics of neurotransmitter transport. *J Bioenerg Biomembr* **30**:173-185.

Rudnick G (2006) Serotonin transporters--structure and function. *J Membr Biol* **213**:101-110.

Rudnick G and Wall SC (1992) The molecular mechanism of "ecstasy" [3,4-methylenedioxy-methamphetamine (MDMA)]: serotonin transporters are targets for MDMA-induced serotonin release. *Proc Natl Acad Sci U S A* **89**:1817-1821.

Russo S, Kema IP, Bosker F, Haavik J and Korf J (2009) Tryptophan as an evolutionarily conserved signal to brain serotonin: molecular evidence and psychiatric implications. *World J Biol Psychiatry* **10**:258-268.

Saier MH, Jr. (2000) A functional-phylogenetic classification system for transmembrane solute transporters. *Microbiol Mol Biol Rev* **64**:354-411.

Sarker S, Weissensteiner R, Steiner I, Sitte HH, Ecker GF, Freissmuth M and Sucic S (2010) The high-affinity binding site for tricyclic antidepressants resides in the outer vestibule of the serotonin transporter. *Mol Pharmacol* **78**:1026-1035.

Schapira M, Abagyan R and Totrov M (2003) Nuclear hormone receptor targeted virtual screening. *J Med Chem* **46**:3045-3059.

Schapira M, Totrov M and Abagyan R (1999) Prediction of the binding energy for small molecules, peptides and proteins. *J Mol Recognit* **12**:177-190.

Schildkraut JJ (1965) The catecholamine hypothesis of affective disorders: a review of supporting evidence. *Am J Psychiatry* **122**:509-522.

Schmid JA, Scholze P, Kudlacek O, Freissmuth M, Singer EA and Sitte HH (2001) Oligomerization of the human serotonin transporter and of the rat GABA transporter 1 visualized by fluorescence resonance energy transfer microscopy in living cells. *J Biol Chem* **276**:3805-3810.

Shan J, Javitch JA, Shi L and Weinstein H (2011) The substrate-driven transition to an inward-facing conformation in the functional mechanism of the dopamine transporter. *PLoS One* **6**:e16350.

Sherman W, Day T, Jacobson MP, Friesner RA and Farid R (2006) Novel procedure for modeling ligand/receptor induced fit effects. *J Med Chem* **49**:534-553.

Shi L, Quick M, Zhao Y, Weinstein H and Javitch JA (2008) The mechanism of a neurotransmitter:sodium symporter--inward release of Na+ and substrate is triggered by substrate in a second binding site. *Mol Cell* **30**:667-677.

Singh SK, Piscitelli CL, Yamashita A and Gouaux E (2008) A competitive inhibitor traps LeuT in an open-to-out conformation. *Science* **322**:1655-1661.

Singh SK, Yamashita A and Gouaux E (2007) Antidepressant binding site in a bacterial homologue of neurotransmitter transporters. *Nature* **448**:952-956.

Sinning S, Musgaard M, Jensen M, Severinsen K, Celik L, Koldso H, Meyer T, Bols M, Jensen HH, Schiott B and Wiborg O (2010) Binding and orientation of tricyclic antidepressants within the central substrate site of the human serotonin transporter. *J Biol Chem* **285**:8363-8374.

Tanford C (1983) Translocation pathway in the catalysis of active transport. *Proc Natl Acad Sci U S A* **80**:3701-3705.

Tate CG (2001) Overexpression of mammalian integral membrane proteins for structural studies. *FEBS Lett* **504**:94-98.

Tate CG, Haase J, Baker C, Boorsma M, Magnani F, Vallis Y and Williams DC (2003) Comparison of seven different heterologous protein expression systems for the production of the serotonin transporter. *Biochim Biophys Acta* **1610**:141-153.

Tatsumi M, Groshan K, Blakely RD and Richelson E (1997) Pharmacological profile of antidepressants and related compounds at human monoamine transporters. *Eur J Pharmacol* **340**:249-258.

Tavoulari S, Forrest LR and Rudnick G (2009) Fluoxetine (Prozac) binding to serotonin transporter is modulated by chloride and conformational changes. *J Neurosci* **29**:9635-9643.

Thompson BJ, Jessen T, Henry LK, Field JR, Gamble KL, Gresch PJ, Carneiro AM, Horton RE, Chisnell PJ, Belova Y, McMahon DG, Daws LC and Blakely RD (2011) Transgenic elimination of high-affinity antidepressant and cocaine sensitivity in the presynaptic serotonin transporter. *Proc Natl Acad Sci U S A* **108**:3785-3790.

Torres-Altoro MI, Kuntz CP, Nichols DE and Barker EL (2010) Structural analysis of the extracellular entrance to the serotonin transporter permeation pathway. *J Biol Chem* **285**:15369-15379.

Vanommeslaeghe K, Hatcher E, Acharya C, Kundu S, Zhong S, Shim J, Darian E, Guvench O, Lopes P, Vorobyov I and Mackerell AD, Jr. (2010) CHARMM general force field: A force field for drug-like molecules compatible with the CHARMM all-atom additive biological force fields. *Journal of computational chemistry* **31**:671-690.

Veber DF, Johnson SR, Cheng HY, Smith BR, Ward KW and Kopple KD (2002) Molecular properties that influence the oral bioavailability of drug candidates. *J Med Chem* **45**:2615-2623.

Walline CC, Nichols DE, Carroll FI and Barker EL (2008) Comparative molecular field analysis using selectivity fields reveals residues in the third transmembrane helix of the serotonin transporter associated with substrate and antagonist recognition. *J Pharmacol Exp Ther* **325**:791-800.

Wang S, Sakamuri S, Enyedy IJ, Kozikowski AP, Deschaux O, Bandyopadhyay BC, Tella SR, Zaman WA and Johnson KM (2000) Discovery of a novel dopamine transporter inhibitor, 4-hydroxy-1-methyl-4-(4-methylphenyl)-3-piperidyl 4-methylphenyl ketone,

as a potential cocaine antagonist through 3D-database pharmacophore searching. Molecular modeling, structure-activity relationships, and behavioral pharmacological studies. *Journal of medicinal chemistry* **43**:351-360.

Wermuth CG, Ganellin, C. R., Lindberg, P., Mitscher, L. A. (1998) Glossary of terms used in medicinal chemistry (IUPAC recommendations 1998). *Pure & Appl Chem* **70**:1129-1143.

White SH (2009) Biophysical dissection of membrane proteins. *Nature* **459**:344-346.

Wolber G, Seidel, T., Bendix, F., Langer, T. (2008) Molecule-pharmacophore superpositioning and pattern matching in computational drug design. *Drug Discovery Today* **13**:23-29.

Yamashita A, Singh SK, Kawate T, Jin Y and Gouaux E (2005) Crystal structure of a bacterial homologue of Na+/Cl--dependent neurotransmitter transporters. *Nature* **437**:215-223.

Yang SY (2010) Pharmacophore modeling and applications in drug discovery: challenges and recent advances. *Drug discovery today* **15**:444-450.

Zhang YW and Rudnick G (2006) The cytoplasmic substrate permeation pathway of serotonin transporter. *J Biol Chem* **281**:36213-36220.

Zhao Y, Terry DS, Shi L, Quick M, Weinstein H, Blanchard SC and Javitch JA (2011) Substrate-modulated gating dynamics in a Na+-coupled neurotransmitter transporter homologue. *Nature* **474**:109-113.

Zhou Z, Zhen J, Karpowich NK, Goetz RM, Law CJ, Reith ME and Wang DN (2007) LeuT-desipramine structure reveals how antidepressants block neurotransmitter reuptake. *Science* **317**:1390-1393.

Zhou Z, Zhen J, Karpowich NK, Law CJ, Reith ME and Wang DN (2009) Antidepressant specificity of serotonin transporter suggested by three LeuT-SSRI structures. *Nat Struct Mol Biol* **16**:652-657.

Zomot E, Bendahan A, Quick M, Zhao Y, Javitch JA and Kanner BI (2007) Mechanism of chloride interaction with neurotransmitter:sodium symporters. *Nature* **449**:726-730.

PAPER 1

PAPER 2

PAPER 3

PAPER 4